ACS OMEGA

Open Access



http://pubs.acs.org/journal/acsodf

Article

# Circular RNA HIPK2 Promotes A1 Astrocyte Activation after Spinal Cord Injury through Autophagy and Endoplasmic Reticulum Stress by Modulating miR-124-3p-Mediated Smad2 Repression

Jin Yang,[†] Junjie Dong,[†] Haotian Li, Zhiqiang Gong, Bing Wang, Kaili Du, Chunqiang Zhang, Hangchuan Bi, Junfei Wang, Xinpeng Tian, and Lingqiang Chen*

Cite This: *ACS Omega* 2024, 9, 781−797

Read Online

ACCESS | Metrics & More | Article Recommendations | Supporting Information

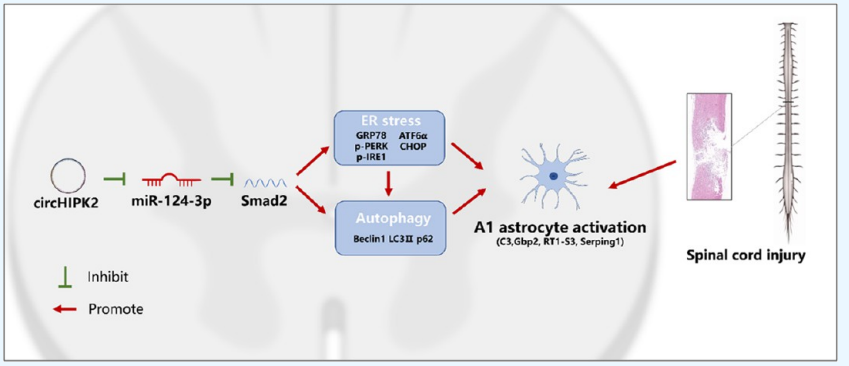


**ABSTRACT:** Glial scarring formed by reactive astrocytes after spinal cord injury (SCI) is the primary obstacle to neuronal regeneration within the central nervous system, making them a promising target for SCI treatment. Our previous studies have demonstrated the positive impact of miR-124-3p on neuronal repair, but it remains unclear how miR-124-3p is involved in autophagy or ER stress in astrocyte activation. To answer this question, the expression of A1 astrocyte-related markers at the transcriptional and protein levels after SCI was checked in RNA-sequencing data and verified using quantitative polymerase chain reaction (qPCR) and Western blotting *in vitro* and *in vivo*. The potential interactions among circHIPK2, miR-124-3p, and Smad2 were analyzed and confirmed by bioinformatics analyses and a luciferase reporter assay. In the end, the role of miR-124-3p in autophagy, ER stress, and SCI was investigated by using Western blotting to measure key biomarkers (C3, LC3, and Chop) in the absence or presence of corresponding selective inhibitors (siRNA, 4-PBA, TG). As a result, SCI caused the increase of A1 astrocyte markers, in which the upregulated circHIPK2 directly targeted miR-124-3p, and the direct downregulating effect of Smad2 by miR-124-3p was abolished, while Agomir-124 treatment reversed this effect. Injury caused a significant change of markers for ER stress and autophagy through the circHIPK2/miR-124-3p/Smad2 pathway, which might activate the A1 phenotype, and ER stress might promote autophagy in astrocytes. In conclusion, circHIPK2 may play a functional role in sequestering miR-124-3p and facilitating the activation of A1 astrocytes through regulating Smad2-mediated downstream autophagy and ER stress pathways, providing a new perspective on potential targets for functional recovery after SCI.

## INTRODUCTION

Spinal cord injury (SCI) is a severe neurotraumatic condition with an annual global incidence estimated at approximately 10.4−83 cases per million individuals and is characterized by irreversible motor, sensory, and autonomous dysfunctions.[1] As per the World Health Organization (https://www.who.int/news-room/fact-sheets/detail/spinal-cord-injury), SCI brings a heavy burden not only to patients but also to the medical system, and the associated costs are much higher than those of comparable neurological diseases such as dementia, multiple sclerosis, and cerebral palsy. SCI involves neuroinflammation, axonal degeneration, neuronal loss, and reactive gliosis. Although therapeutic strategies aimed at enhancing tissue repair and neuroplasticity have shown achievement to some extent, there is still a lack of effective approaches aiming at neuronal repair and regeneration for SCI treatment as both intrinsic factors and extrinsic environmental factors for injury. Therapeutic approaches aiming at glial cells specifically have been proposed to gain timely control of the glial activation and

Received: September 5, 2023
Revised: November 10, 2023
Accepted: November 24, 2023
Published: December 26, 2023

scar formation processes to unravel the regeneration potential of the neurons after SCI.[2]

Astrocytes, which are the principal type of glial cells found in the central nervous system (CNS), play various roles and have different functions, including the secretion of neurotrophic mediators,[3] proinflammatory factors, and cytotoxic agents. After the onset of SCI, violently activated astrocytes present in the injured region are termed reactive astrocytes, including neurotoxic A1 type and neuroprotective A2 type. A1 astrocytes become hypertrophic and promote the formation of a glial scar; the scar not only seals the lesion areas to prevent the spread of injury-related molecules to neighboring tissues but also exerts detrimental effects by impeding axonal regeneration after SCI[4,5] through the production of axonal growth inhibitors and by shutting off conducive signaling transmission.[5,6] Failure in glial scar formation exacerbates tissue damage and triggers axonal degeneration.[7] Thus, considering the specific process of astrocyte polarization in various diseases,[8] further therapeutic manipulation in terms of the plasticity of the reactive astrocytes involved in astrogliosis that can block the inhibition of axonal repair without compromising the protecting role holds a high potential for future astrocyte-based therapy for SCI.[4,9,10] A1 astrocytes are responsible for the secretion of inflammatory and neurotoxic factors.[11] The neurotoxicity function of A1 astrocytes is meaningfully inhibited with tumor necrosis factor (TNF)-$\alpha$, C1q inhibitors, and interleukin (IL)-1$\alpha$ to promote axonal regeneration and hinder optic ganglion cell necrosis.[10] A1 astrocytes are capable of inducing the death of neuronal cells and oligodendrocytes as well as destroying synapses. These processes are triggered by activated neuroinflammatory microglia.[11,12] Neuroreactive astrocytes induce neurotoxicity through saturated lipids and then trigger neuronal cell death.[12] Conversely, A2 astrocytes can be activated in response to ischemia, exhibiting a beneficial impact on protecting the nervous system, facilitating tissue repair and regeneration.[11] The expression of distinct transcripts in A1 and A2 astrocytes, along with their respective roles in various diseases or injuries, has been documented.[4,13] The modulation of A1/A2 astrocyte activation and conversion between the A1 and A2 types are recently emerging targets for the treatment of CNS diseases or injuries.[14−16] Therefore, in this study, we focus on the regulation of astrocyte polarization.

micro-RNA 124-3p (miR-124-3p), one of the essential dysregulated miRNAs after SCI, has been well studied owing to its therapeutic potential in neurodegenerative disorders and SCI.[17] Consistently, other previous studies, including ours, have shown the decreased expression of miR-124-3p in the injured sites or the peri-lesion area after SCI.[18,19] Injection of miR-124 can not only reduce the scar area formed by astrocytes but also affect immune cells and microglia.[20] Agomir-124 treatment also inhibits astrocyte proliferation and reactivity after SCI and downregulates GFAP expression,[21] in which the autophagy and endoplasmic reticulum (ER) stress pathway may be involved.[22] miR-124-3p is also enriched in neuron-derived exosomes transported from neurons to astrocytes through vesicles to exert a neuroprotective function.[23,24] miR-124-3p promotes the infiltration of reactive astrocytes into the lesion and decreases the extent of glial scars mainly formed by astrocytes to increase the survival of neurons and promote functional improvement in neurological deficits.[25] miR-124-3p has the potential to induce A1 astrocytes through its suppression of the myosin heavy chain 9 (MYH9)/PI3K/AKT/NF-$\kappa$B signaling cascade, thus promoting functional recovery in mouse models after SCI.[24] These findings cumulatively highlight the roles of miR-124-3p in regulating A1 astrocytes, but the underlying mechanisms remain unexplored.

Circular ribonucleic acid (circRNA) is a newly discovered type of noncoding RNA that possesses a unique structure, consisting of a single-stranded, closed-loop shape devoid of caps at the 5′ end or poly A tails at the 3′ end.[26] Given that circRNA is aberrantly expressed after SCI onset, it has become a research hotspot as a therapeutic option or biomarker for SCI.[27] As for the regulatory roles of circRNAs, they serve as sponges of miRNAs, directly regulate target gene transcription, and enhance translation into proteins.[28] SCI causes the overactivation of astrocytes. The identification and analysis of the interaction network involving circRNA−miRNA−mRNA are imperative for elucidating the pathogenesis of diseases related to astrocytes and for providing essential guidance in the treatment of SCI.[29] In the present study, we screened for circRNAs with up- and downregulated expressions and correlated them with the miR-124-3p sponging effect. Additionally, the expression of A1 astrocyte-related markers (Gbp2, RT1-S3, SerpinG1, and C3) after SCI was examined to understand the effect of miR-124-3p on the spinal cord astrocyte function in SCI, and the effects of Agomir-124 treatment on the activation of A1 astrocytes were verified *in vitro* and *in vivo*.

## MATERIALS AND METHODS

**SCI Procedure.** Sprague-Dawley rats (body weight: 200−250 g) were obtained from Shanghai SLAC Laboratory Animal Co., Ltd. (Shanghai, China). The Animal Experimental Ethics Committee of Kunming Medical University approved the protocols of this study (approval no.: kmmu2020462), adhering to the guidelines for laboratory animals. The rats were first deeply anesthetized with 4% inhalant isoflurane and then subjected to contusion SCI using a weight drop apparatus at the 10th thoracic vertebral (T10) level. Briefly, the animals underwent T10 laminectomy to expose the spinal cord segment; subsequently, they were exposed to a spinal cord impactor device (RWD Life Science, Shenzhen, China; 1 m/s speed, 2 mm depth, 1 s dwell time) and underwent weight drop from a 10 g steel rod placed at a height of 50 mm. In the SCI+Agomir-124 group, rats were administered an intrathecal injection of agomiR-124 (20 $\mu$M, encapsulated in liposomes) in a volume of 5 mL. In the SCI+Agomir-NC group, rats were subjected to negative control (NC) treatment 24 h post SCI induction. The sham group, composed of rats that underwent laminectomy without any subsequent injury, served as the control group. After surgery, animals urinated from their bladders and received painkiller injections for 3 consecutive days. Behavioral evaluation of locomotor impairment was performed by using the Basso, Beattie, and Bresnahan score.

**Hematoxylin−Eosin Staining.** At the end of the corresponding treatment, all of the rats were euthanized by administering a lethal overdose of 2% pentobarbital sodium (120 mg/kg; injected intraperitoneally). A spinal cord tissue section of 2 mm thickness present outside the injury center was collected and then fixed. After fixation, the tissue section containing the lesion was embedded with paraffin, after which it was sliced into sections that were 5 $\mu$m thick. Some of these sections were fixed with 10% formalin for 2 days for histopathological analysis (hematoxylin−eosin staining), and the remaining tissue sections were preserved at a temperature of −80 °C for further experiments. The tissue sections of the


https://doi.org/10.1021/acsomega.3c06679
ACS Omega 2024, 9, 781−797

spinal cord embedded in paraffin were dewaxed by using xylene and alcohol. The slides were sequentially soaked in hematoxylin for 5 min, 2% glycolic acid, and lithium carbonate. The slides were then soaked in eosin for 2 min, after which they were dehydrated with ethanol before xylene. The SCI area was measured using ImageJ software.

**Library Construction and circRNA Sequencing.** TRIzol reagent (Invitrogen, Carlsbad, CA, USA) was employed to extract the total RNA from the injured. RNA quality was assessed by employing standard denaturing 1% agarose gel electrophoresis. The assessment of RNA integrity was conducted on the Bioanalyzer 2100 system by Agilent Technologies in Santa Clara, CA, utilizing the RNA Nano 6000 Assay Kit. The construction of the RNA library and sequencing of circRNAs were performed at Nuohe Zhiyuan Technology (Beijing, China). The input material for RNA sample preparation consisted of 5 $\mu$g of RNA per sample. In order to enhance the abundance of and reduce the levels of rRNAs, the total RNA was subjected to digestion using RNase R (Epicenter, Madison, WI, USA) and depletion using the Ribo-Zero Magnetic Gold Kit (Epicenter). And the RNA libraries were prepared with rRNA-depleted RNAs, using the TruSeq Stranded Total RNA Library Prep Kit from Illumina (San Diego, CA, USA), in accordance with the protocols provided by the manufacturer. The quality and quantity of the constructed libraries were verified using the BioAnalyzer 2100 system. The libraries were then converted to single-stranded DNA molecules, which were then captured on Illumina Flow Cells. After being amplified on-site in clusters, they were eventually sequenced for 150 cycles using the HiSeq 4000 Sequencing System manufactured by Illumina.

**Isolation of Primary Astrocytes.** The primary astrocytes from the spinal cord tissues were isolated from newborn Sprague-Dawley rats (aged 1−5 days), after which the tissues were dissected, minced, and digested according to the method described previously.[30] Dulbecco's modified Eagle's medium (DMEM; Gibco, Life Technologies, Grand Island, NY, USA) with the addition of 10% fetal bovine serum (FBS; BI, Israel) was used to stop digestion. Afterward, the entire solution was passed through a 30 $\mu$m nylon mesh, and the resulting filtrate was centrifuged at 1200 rpm for 5 min. The dissociated cell populations were resuspended and washed twice, followed by seeding into culture dishes that had been pretreated with poly-L-lysine (Thermo Scientific, Roskilde, Denmark), containing DMEM supplemented with 10% FBS and 1% penicillin−streptomycin (Gibco). The medium was replenished every 2−3 days until the cells reached confluence (∼10 days). Nonastrocytes were detached by agitation in a 37 °C incubator at 200 rpm overnight and then removed by replenishing the medium. The astrocytes were evaluated by positive staining using the astrocytic marker glial fibrillary acid protein (GFAP) in order to evaluate their presence or activation. Astrocytes with more than 95% purity were readily used for subsequent experiments after 2−3 passages. The A172 cell line of human astrocytes (ATCC) was cultured in DMEM, with the addition of 10% FBS, 2.5 mM L-glutamine (Invitrogen), and 0.3 mg/mL Geneticin (Gibco), in a humidified incubator under standard conditions of 37 °C temperature and 5% $CO_2$ concentration.

We used scratched astrocytes as the SCI model *in vitro*. For the scratch wound assay, the cell monolayer was scraped using a pipet tip head to form a linear wound of 200 $\mu$m width.[31,32] The inhibitor and activator of ER stress, namely, 4-phenyl butyric acid (4-PBA) and thapsigargin (TG), respectively, as well as the autophagy modulators, 3-MA and rapamycin, were obtained from Sigma-Aldrich (St. Louis, MO, USA). Primers for miR-124-3p mimic, miR-124-3p inhibitor, si-circHIPK2, si-Smad2, U6, and $\beta$-actin were purchased from GenePharma (Shanghai, China).

**Western Blot Analysis.** The spinal cord tissue was homogenized with a buffer (KeyGen Biotechnology, Nanjing, China), and the extraction of total protein was accomplished using the radioimmunoprecipitation assay buffer (RIPA lysis buffer). After the determination of total protein concentration (the bicinchoninic acid method), 40 $\mu$g of total protein was considered for subsequent experiments. Later, samples containing equivalent protein quantities were separated through sodium dodecyl sulfate polyacrylamide gel electrophoresis (SDS-PAGE) and then transferred onto poly(vinylidene difluoride) membranes (EMD Millipore Corp, Burlington, MA, USA). The membranes were obstructed with bovine serum albumin (BSA) at a concentration of 5% (v/v) and subsequently incubated overnight at a temperature of 4 °C with primary antibodies. Afterward, the membranes were subsequently subjected to a 2 h incubation with the secondary antibody at room temperature. The immunolabeled bands were observed by utilizing an enhanced chemiluminescence reagent (Thermo Fisher Scientific), and the expression levels of the target protein bands were semiquantified utilizing ImageJ, a software provided by the National Institutes of Health, located in Bethesda, MD, USA. Relevant antibody information for the Western blot assay in this study were as follows: anti-GAPDH (1:10000 dilution, rabbit, ab181602; Abcam, Cambridge, U.K.), anti-GFAP (1:2000 dilution, mouse, ab4648; Abcam), anti-C3 (1:1000 dilution, rabbit, ab97462; Abcam), anti-LC3B (1:2000 dilution, rabbit, ab48394; Abcam), anti-Smad2 (1:1000 dilution, mouse, ab119907; Abcam), anti-Beclin-1 (1:1000 dilution, rabbit, ab62557; Abcam), anti-p62 (1:1000 dilution, rabbit, ab91526; Abcam), anti-GRP78 (1:1000 dilution, rabbit, ab21685; Abcam), anti-p-IRE1$\alpha$ (1:1000 dilution, rabbit, ab48187; Abcam), anti-IRE1$\alpha$ (1:1000 dilution, rabbit, ab37073; Abcam), anti-p-PERK (1:500 dilution, sc-32577, rabbit; Santa Cruz Biotechnology, Dallas, TX), anti-PERK (1:500 dilution, sc-13073, rabbit; Santa Cruz Biotechnology), anti-ATF6 (1:1000 dilution, rabbit, ab62576; Abcam), and anti-CHOP (1:2000 dilution, mouse, ab11419; Abcam). The secondary antibodies included goat antimouse Alexa Fluor 488 (1:1000 dilution, goat, ab150113; Abcam), goat antirabbit Alexa Fluor 594 (1:1000 dilution, goat, ab150088; Abcam), goat antimouse Alexa Fluor 594 (1:1000 dilution, goat, ab150120; Abcam), and goat antirabbit Alexa Fluor 488 (1:1000 dilution, goat, ab150077; Abcam).

**Reverse Transcription-Quantitative Polymerase Chain Reaction.** Total RNA from injured tissues of the rat spinal cord and the astrocytes was extracted, manufactured by TRIzol reagent. A reverse transcription system (Toyobo, Osaka, Japan) was employed for the synthesis of complementary DNA, while the ABI 7900 fast real-time PCR system (Applied Biosystems, Carlsbad, CA, USA) was utilized for performing quantitative polymerase chain reaction (qPCR) using the SYBR Green PCR master mix (Applied Biosystems). The relative expression levels of the target genes were assessed by utilizing the $2^{-\Delta\Delta Ct}$ method after standardizing them to $\beta$-actin or U6.

**Luciferase Reporter Assay.** GeneScript (Nanjing, China) synthesized the sequences that contained wild-type (WT) or


https://doi.org/10.1021/acsomega.3c06679
ACS Omega 2024, 9, 781−797

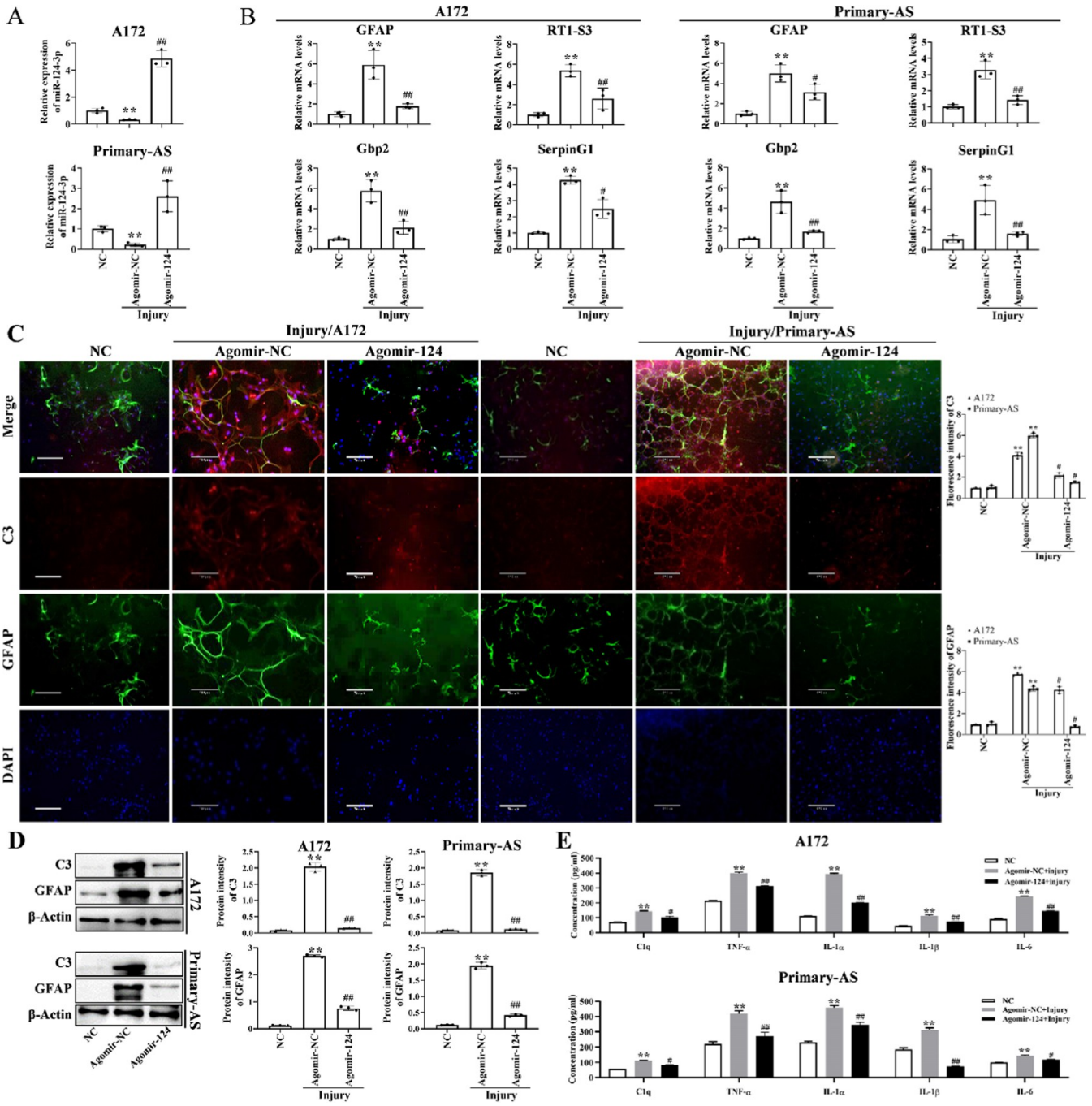


**Figure 1.** Agomir-124 inhibits the activation of A1 astrocytes *in vitro*. (A) miR-124-3p expression in an injury model of primary astrocytes and an astrocyte cell line. (B) RT-qPCR analysis of differential expression of astrocyte markers in an injury model of primary astrocytes and astrocyte cell line. (C) Colocalization of C3 and GFAP in an injury model of two cell types. Green, GFAP; red, C3; blue, DAPI. Scale bar: 100 $\mu$m. (D) WB analysis of C3 and GFAP expression in an injury model of two cell types. (E) ELISA assay measurement of proinflammatory cytokines induced by the injury of two cell types. Mean ± SD, $n$ = 3, $^{**}P < 0.01$, compared to NC group; $^{\#}P < 0.05$, $^{\#\#}P < 0.01$, compared to Agomir-NC group. C3, complement component 3; DAPI, 4′,6-diamidino-2-phenylindole; ELISA, enzyme-linked immunosorbent assay; GFAP, glial fibrillary acid protein; RT-qPCR, reverse transcription−quantitative polymerase chain reaction; miR, micro-RNA; WB, Western blotting; SD, standard deviation.

mutant (MUT) miR-124-3p binding sequences corresponding to the 3′-untranslated region (UTR) of Smad2 mRNA. Afterward, these sequences were cloned into the pGL3 luciferase control reporter vector (Promega, Madison, WI, USA), using the *Fse*I and *Xba*I restriction sites, allowing the generation of the 3′-UTR reporter constructs of Smad2 (WT-Smad2 and MUT-Smad2).

Astrocytes were then seeded in 24-well plates, followed by a 24 h incubation, after which they were subjected to transfection. The transfected astrocytes, which were either treated with miR-124-3p mimic or NC, were then placed into 96-well plates and cotransfected with either WT-Smad2 or MUT-Smad2 using a dose of 10 ng. Firefly and Renilla luciferase signals were measured by employing the Dual-Luciferase Assay Kit (Promega).


https://doi.org/10.1021/acsomega.3c06679
*ACS Omega* 2024, 9, 781−797

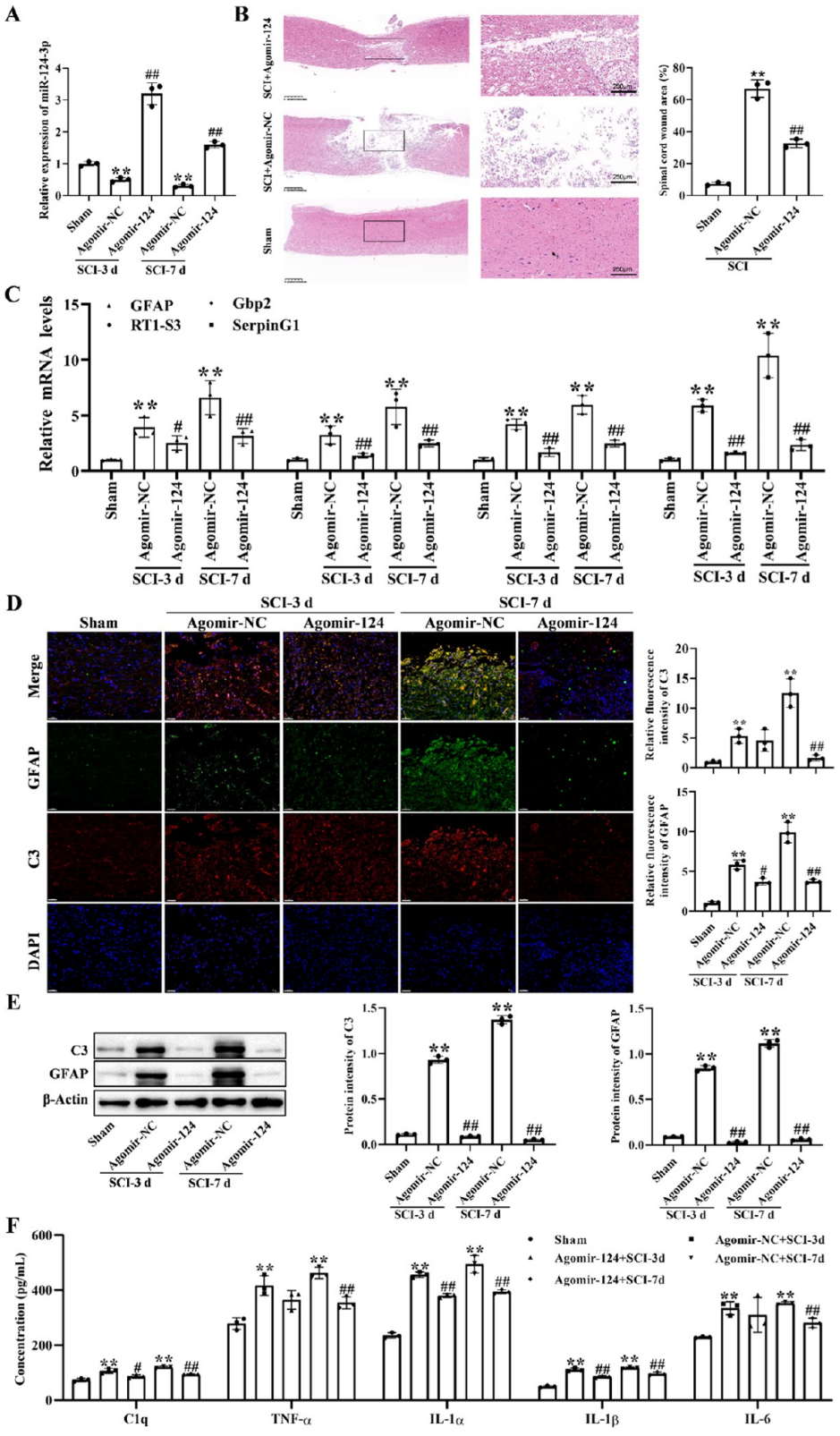


**Figure 2.** Agomir-124 inhibits the activation of A1 astrocytes *in vivo*. (A) miR-124-3p expression at the site of injury at 3 and 7 dpi. (B) Representative hematoxylin−eosin staining image at 7 dpi. (C) RT-qPCR analysis of A1 astrocyte markers at the site of injury at 3 and 7 dpi. (D) Colocalization of C3 and GFAP at the site of injury at 3 and 7 dpi, with the scale bar measuring 50 $\mu$m. (E) WB analysis of C3 and GFAP expression at the injury site at 3 and 7 dpi. (F) ELISA assay measurement of proinflammatory cytokines at the injury site at 3 and 7 dpi. Mean ± SD, $n = 3$. $^{**}P < 0.01$, compared to sham group; $^{\#}P < 0.05$, $^{\#\#}P < 0.01$, compared to Agomir-NC group. C3, complement component 3; GFAP, glial fibrillary acid protein; RT-qPCR, reverse transcription−quantitative polymerase chain reaction; ELISA, enzyme-linked immunosorbent assay; miR, micro-RNA; WB, Western blotting; SD, standard deviation.



https://doi.org/10.1021/acsomega.3c06679
*ACS Omega* 2024, 9, 781−797

**Immunofluorescence Staining.** Spinal cord tissue segments were fixed using a 4% paraformaldehyde solution overnight, followed by dehydration in 15 and 30% sucrose solutions to make frozen samples. The frozen-embedded spinal cord segments were then sliced into sections that were 10 mm thick for utilization in further experiments. To carry out immunofluorescence staining on the tissues, the sections were blocked using a 10% BSA solution and incubated with the primary antibodies overnight at 4 °C, namely, anti-GFAP (rabbit, ab278054; Abcam) and anti-C3 (rabbit, ab97462; Abcam). Subsequently, the membrane was incubated at room temperature for a duration of 1 h with the application of secondary antibodies. To conduct cellular immunofluorescence staining, briefly, the astrocytes underwent a 30 min fixation, a permeability with 0.05% Triton X-100, and a blocking with 5% BSA. The primary antibodies were used for specific binding of GFAP and C3 proteins once again, followed by subsequent incubation with secondary antibodies. The tissues were washed three times with phosphate-buffered saline before counterstaining the nuclei with 4′,6-diamidino-2-phenylindole (DAPI; Thermo Fisher Scientific). Representative immunostaining images were captured on day 3 post injury as well as the images of the GFAP and C3 in the injured spinal cord lesion areas were captured on day 7 post injury. Fluorescence images were obtained by using the ImagerA2 fluorescence microscope.

**Enzyme-Linked Immunosorbent Assay.** To assess the alternatives on inflammatory cytokines, C1q, TNF-$\alpha$, IL-1$\alpha$, IL-1$\beta$, and IL-6 expression levels, the tissues were isolated 3 days after the onset of SCI. The homogenizer was used to homogenize the SCI tissue, and the resulting homogenate was then stored in liquid nitrogen. In addition, lysis buffer, which contained 1 mM ethylenediamine tetraacetic acid (EDTA), 1% Triton X-100, 1 mM phenylmethylsulfonyl fluoride, 10 mM tris (pH 8.0), 150 mM NaCl, and 5 $\mu$L/mL protease inhibitor, was added to the lysates, after which the resulting solution was subjected to incubation at 4 °C for a duration of 1 h. The lysates were subject to centrifugation at a speed of 3000 rpm for a duration of 30 min. The supernatants collected were analyzed through the utilization of enzyme-linked immunosorbent assay (ELISA) kits to quantify the concentration of cytokines, in accordance with the guidelines provided by the manufacturer. The levels of proinflammatory cytokines were assessed in the astrocyte culture medium through the utilization of ELISA kits, following the established protocols provided by the manufacturer. The measurement of optical density or fluorescence was conducted through the utilization of a plate reader device. ELISA kits could detect TNF-$\alpha$ (MTA00B; R&D), IL-1$\alpha$ (MLA00; R&D), IL-1$\beta$ (MLB00C; R&D), IL-6 (M6000B; R&D), and C1q (HK211; Hycult Biotech).

**Statistical Analysis.** Experiments were conducted with a minimum of three distinct biological replicates. The data were presented as the mean ± standard deviation. Statistical analysis was carried out using GraphPad software version 8.0 and SPSS version 25.0. Student's $t$ test was utilized for comparing two groups, while one-way or two-way analysis of variance was employed for comparing more than two groups. The $P$-values were used to calculate statistical significance, with $P < 0.05$ considered as indicative of significance.

## RESULTS

**Astrocyte-Specific Transcripts Increase after SCI.** RNA-Seq experiments were performed on spinal cord tissues to identify the astrocyte transcriptome expression profiles. DE mRNAs were identified, wherein 210 genes were upregulated and 78 genes were downregulated in the SCI group when compared with those of the sham group at 7 days post injury (dpi; Table S1). Among the astrocyte-specific transcripts, when compared with the sham group, those with significantly upregulated expression included PAN-reactive-related genes (Vim, Timp1, and GFAP) and A1 astrocyte-specific genes (SerpinG1, C3, Gbp2, and RT1-S3). Simultaneously, pronounced variations were discerned in A2 astrocyte-specific genes (Emp1, S100a10, Clcf1, and Ptgs2) within the SCI group; however, no notable disparities were detected in the Ggm1 gene.

**Effect of miR-124-3p on A1 Astrocyte Polarization Markers *In Vitro*.** Next, we evaluated representative genes in both the A172 astrocyte cell line and primary cultured astrocytes through the scratch wound assay *in vitro*. miR-124-3p levels were reduced 24 h after inducing the scratch, which were then rescued by Agomir-124 treatment in both cell types (Figure 1A). The PAN-reactive transcripts of glial fibrillary acid protein (GFAP) and A1-specific markers (Gbp2, RT1-S3, and SerpinG1) in the injury group were remarkably enhanced compared to those in the NC group, which markedly decreased with Agomir-124 treatment (Figure 1B). Similarly, according to the immunofluorescence staining and Western blotting results, C3 (a specific marker for A1) and GFAP showed a remarkable increase in the injury group compared to the NC group. However, after treatment with Agomir-124, these levels were significantly reduced in both cell types (Figure 1C,D). Additionally, enzyme-linked immunosorbent assay (ELISA) results showed that SCI could induce the production of inflammatory cytokines, including C1q, TNF-$\alpha$, IL-1$\alpha$, IL-1$\beta$, and IL-6, whereas Agomir-124 treatment inhibited the induction of these factors (Figure 1E).

**Effect of miR-124-3p on Astrocyte Polarization Markers *In Vivo*.** The effect of miR-124-3p on the A1 astrocyte-type conversion was validated *in vivo*. miR-124-3p expression after spinal cord contusion at 3 and 7 days showed a reduction in comparison to the sham group, which was rescued by Agomir-124 treatment (Figure 2A). The application of Agomir-124 reduced the wound area by 7 days (Figure 2B). The transcript levels of GFAP and A1-specific markers (Gbp2, RT1-S3, and SerpinG1) were upregulated at 3 and 7 days (Figure 2C), which were reduced by Agomir-124 treatment. The immunofluorescence results indicate an upregulation of both C3 and GFAP in the group with SCI at 3 and 7 dpi. It is important to note that following treatment with Agomir-124, there was significant decreases in GFAP expression at both 3 and 7 dpi. Although no significant changes in C3 expression were observed at 3 dpi after Agomir-124 treatment compared to the SCI group, a significant decrease in C3 expression was observed at 7 dpi (Figure 2D). Western blot analysis of GFAP and C3 expression at 3 and 7 days showed a relatively weak expression in the Agomir-124 group in comparison to that in the SCI group (Figure 2E). ELISA results showed that SCI promoted the production of inflammatory cytokines, including C1q, IL-6, IL-1$\alpha$, IL-1$\beta$, and TNF-$\alpha$, whereas Agomir-124 inhibited the production of these factors (Figure 2F), which are consistent with the *in vitro* results. The obtained results unequivocally substantiated the suppressive role exerted by miR-124-3p in the conversion of astrocytes into the A1 type after SCI both *in vitro* and *in vivo*.


https://doi.org/10.1021/acsomega.3c06679
ACS Omega 2024, 9, 781−797

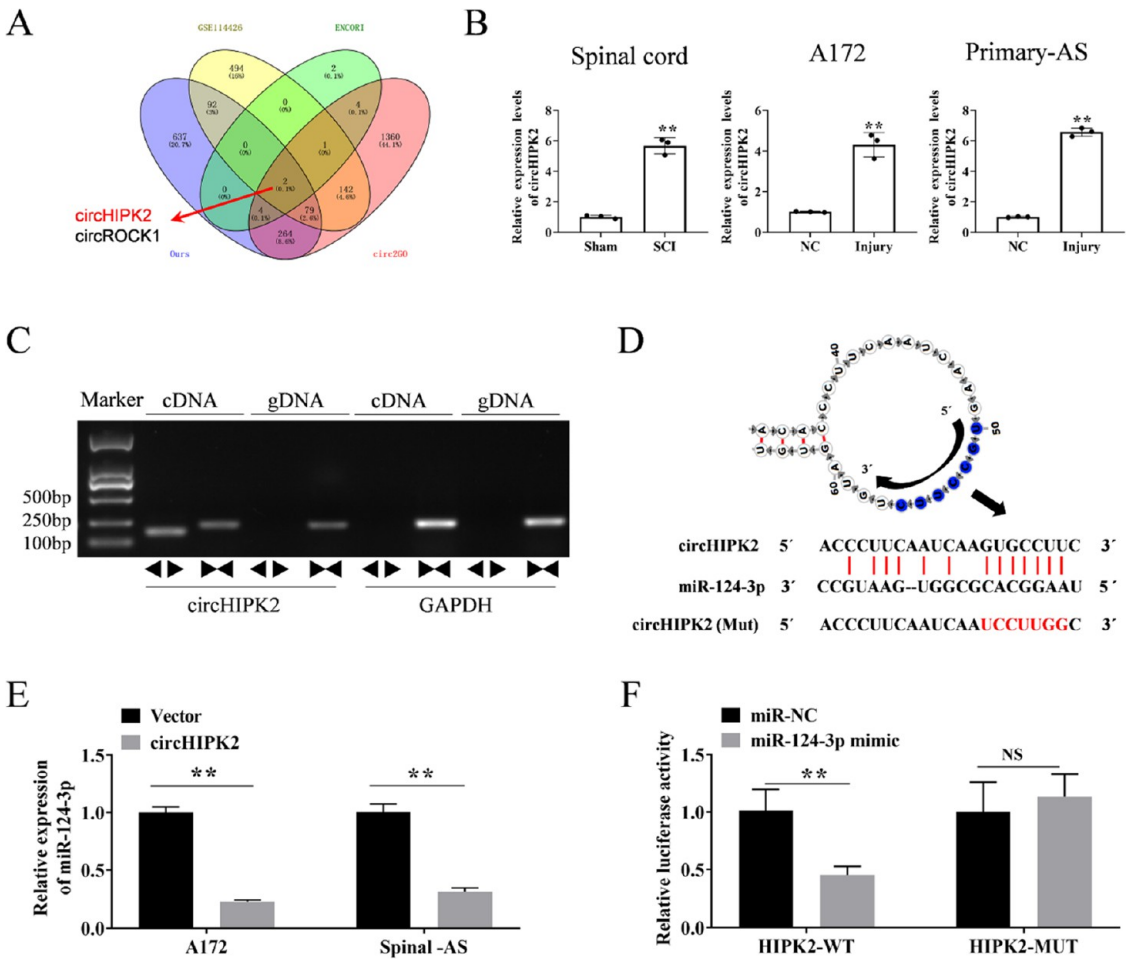


**Figure 3.** circHIPK2 targets miR-124-3p in A1 astrocyte activation after SCI. (A) Venn diagram analysis shows the upregulated expression of circRNAs when targeting miR-124-3p after SCI. (B) Validation of the upregulated circHIPK2 expression *in vivo* and *in vitro*. (C) Divergent primers are used for amplifying the circRNAs in cDNA but not in genomic DNA by RT-qPCR. GAPDH, linear control. (D) Binding site between circHIPK2 and miR-124-3p. (E) Effect of circHIPK2 on miR-124-3p expression in two cell types. (F) Dual-luciferase reporter system is used for the detection of the fluorescence efficiency of cotransfected circHIPK2 (circHIPK2-WT) or its mutant (circHIPK2-Mut) with the miR-124-3p mimic and miR-NC. All groups had three biological replicates, and all reactions were executed in triplicate. Mean ± SD, $n = 3$, $^{**}P < 0.01$. cDNA, complementary DNA; circRNA, circular RNA; SCI, spinal cord injury; RT-qPCR, reverse transcription−quantitative polymerase chain reaction; GAPDH, glyceraldehyde 3-phosphate dehydrogenase; miR, micro-RNA; NC, negative control; WT, wild type; SD, standard deviation.

**circHIPK2 Targets miR-124-3p in Astrocytes.** A total of 810 DE-circRNAs were screened from the microarray GEO database (https://www.ncbi.nlm.nih.gov/geo/) in GSE114426 (three pairs of rat SCI and sham tissues) with a multiple of change of >1.5. Our circRNA sequencing data indicated that 1087 circRNAs had upregulated expression in the SCI group, as compared to that in the sham group (Table S2). Using online tools, including ENCORI (http://starbase.sysu.edu.cn/) and circ2GO (https://circ2go.dkfz.de/), we identified 1477 and 2069 circRNAs that potentially interact with miR-124-3p, respectively (Table S2). Finally, two circRNAs were obtained, namely, circHIPK2 and circROCK1 (Figure 3A). circHIPK2 is upregulated in the SCI models (Figure 3B). circHIPK2 expression was verified by using diverse primers (Figure 3C). The results of the analysis performed in the ENCORI database, showing the prediction of targeting sequences between miR-124-3p and circHIPK2, can be seen in Figure 3D. circHIPK2 overexpression downregulated miR-124-3p expression in primary astrocytes and the A172 cell line (Figure 3E). A dual-luciferase reporter assay confirmed that miR-124-3p binds to circHIPK2, as the luciferase activity of circHIPK2-WT significantly decreased in the miR-124-3p mimic group, with no significant differences in the luciferase activities of cells cotransfected with circHIPK2-MUT and miR-124-3p mimic (Figure 3F).

**circHIPK2/miR-124-3p Is Probably Involved in Astrocyte Activation during an Injury *In Vivo* and *In Vitro*.** Given that A1 astrocytes were overactivated during injury under *in vivo* and *in vitro* conditions, we speculated that it might be mediated by miR-124-3p. We evaluated whether circHIPK2/miR-124-3p is involved in the activation of the A1 astrocytes. The knockdown expression of si-circHIPK2 was detected in Figure S1. Compared to the NC group, circHIPK2 increased the levels of the A1 marker C3 in astrocytes of the injury model for two types of astrocyte cells (*in vitro*) after injury, and SCI models (*in vivo*), but si-circHIPK2 reduced C3 levels both *in vitro* and *in vivo* (Figure S2). Furthermore, the Smad2 level increased at both transcriptional and translational levels after injury but showed significant downregulation with the Agomir-124 treatment (Figure S3).

**circHIPK2/miR-124 Probably Targets and Regulates Smad2 in the Activation of A1 Astrocytes.** When


https://doi.org/10.1021/acsomega.3c06679
ACS Omega 2024, 9, 781−797

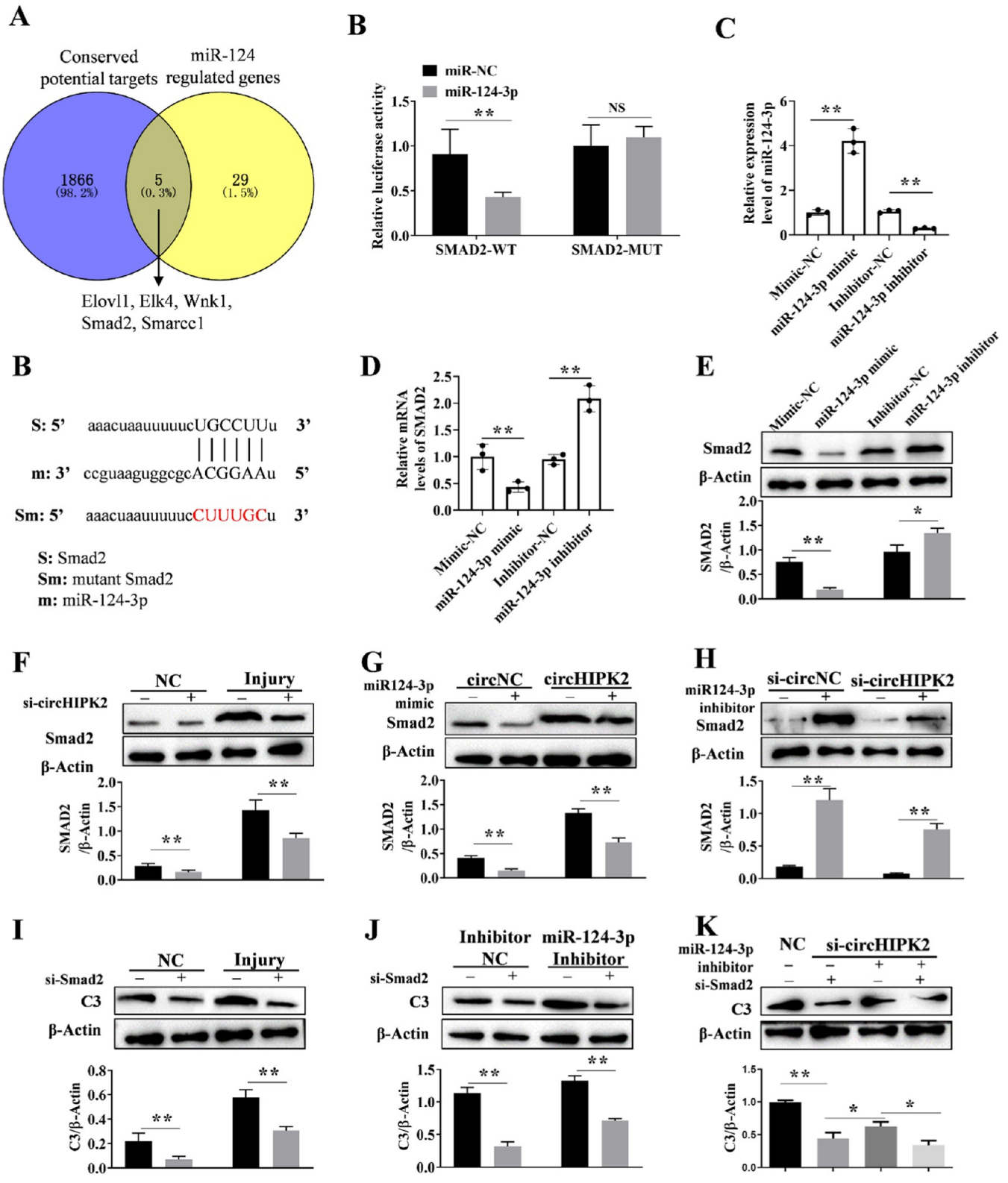


**Figure 4.** circHIPK2/miR-124 targets and regulates the participation of Smad2 in the activation of A1 astrocytes. (A) Venn diagram analysis shows that Smad2 targets miR-124-3p and demonstrates upregulated expression after SCI but downregulated expression with Agomir-124 treatment. (B) Binding sites between Smad2 and miR-124-3p. (C) Dual-luciferase reporter system for the detection of the fluorescence efficiency of cotransfected Smad2 (Smad2-WT) or its mutant (Smad2-Mut) with the miR-124-3p mimic and miR-NC. (D) RT-qPCR analysis of the efficiency of the miR-124-3p mimic- and miR-124-3p inhibitor-transfected cells. (E, F) Smad2 expression at the mRNA and protein levels in miR-124-3p-OE- and si-miR-124-3p-transfected A172 cells. (G) Effects of miR-124-3p on Smad2 expression after circHIPK2 siRNA transfection in the astrocyte cell line A172. (H−K) Relative protein levels of Smad2 and C3 with the indicated treatments in the astrocyte cell line A172. Mean ± SD, $n = 3$, $^{*}P < 0.05$; $^{**}P < 0.01$. C3, complement component 3; RT-qPCR, reverse transcription−quantitative polymerase chain reaction; miR, micro-RNA; NC, negative control; SCI, spinal cord injury; SD, standard deviation; siRNA, small interference RNA; WT, wild type.



https://doi.org/10.1021/acsomega.3c06679
ACS Omega 2024, 9, 781−797

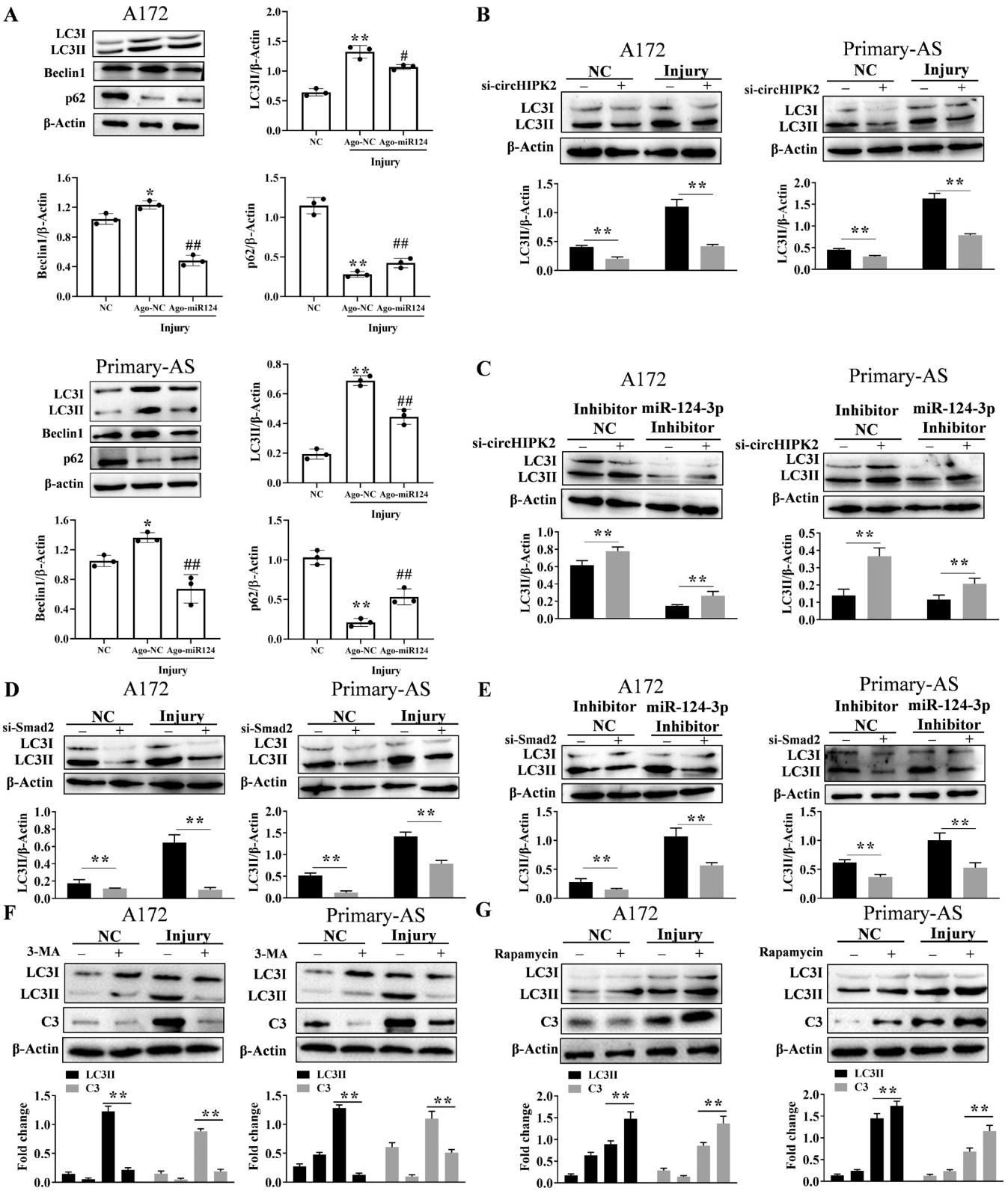


**Figure 5.** circHIPK2/miR-124-3p/Smad2 promotes the activation of A1 astrocytes through autophagy. (A) Protein levels of LC3II, Beclin-1, and p62 expression in two astrocyte cells. *$P < 0.05$, **$P < 0.01$, compared to the sham group; ##$P < 0.01$, compared to the Agomir-NC group. (B−E) Relative protein levels of LC3II with indicated treatments in two cell types. (F−G) Relative protein levels of C3 and LC3II in two cell types after treatment with an autophagy activator and an autophagy inhibitor for 24 h after injury. Mean ± SD, $n = 3$, **$P < 0.01$. C3, complement component 3; miR, micro-RNA; SD, standard deviation.

comparing the sequencing data, 34 genes had an upregulated expression in the SCI group (vs sham group) but had a downregulated expression in the Agomir-124 treatment group (vs SCI group; Table S3), and five genes were identified:



https://doi.org/10.1021/acsomega.3c06679
ACS Omega 2024, 9, 781−797

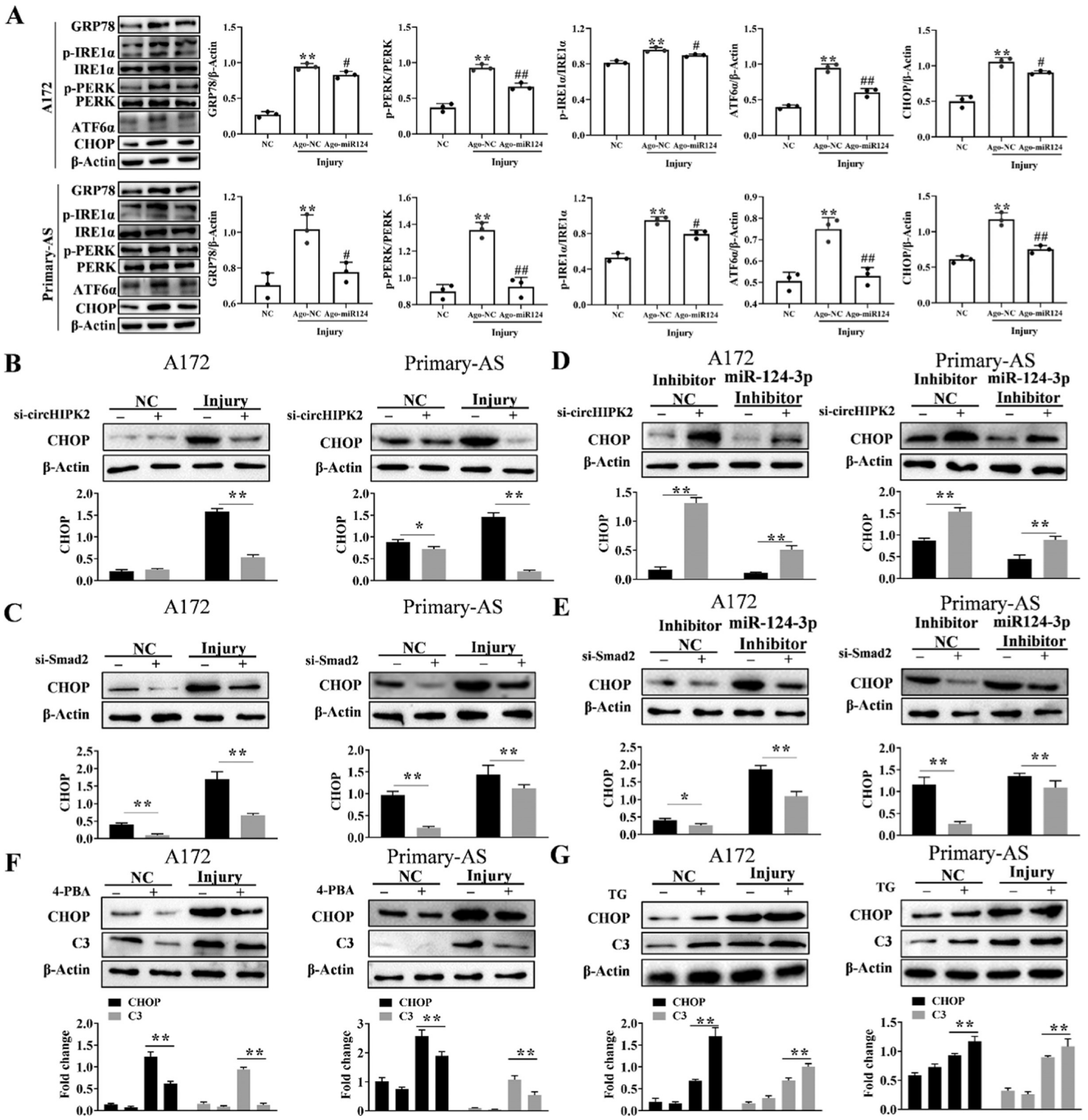


**Figure 6.** circHIPK2/miR-124-3p/Smad2 regulates ER stress in the activation of A1 astrocytes. (A) Protein levels of GRP78, ATF6$\alpha$, CHOP, p-IRE1$\alpha$/IRE1$\alpha$, and p-PERK/PERK in two astrocyte cells. $^{*}P < 0.05$, $^{**}P < 0.01$, compared to the sham group; $^{\#}P < 0.05$, $^{\#\#}P < 0.01$, compared to the Agomir-NC group. (B−E) Relative protein levels of CHOP with the indicated treatments in two cell types. (F−G) Relative protein levels of C3 and CHOP in two cell types after treatment with an ER stress activator and an ER stress inhibitor for 24 h post injury. $^{*}P < 0.05$; $^{**}P < 0.01$. C3, complement component 3; ER, endoplasmic reticulum; miR, micro-RNA.

Elovl1, Elk4, Wnk1, Smad2, and Smarcc1n (Figure 4A). Among them, Smad2, which is targeted by miR-124-3p, serves as a downstream molecule mediating transforming growth factor $\beta$ (TGF-$\beta$) signals. The results of RT-qPCR and Western blotting assays suggested that Agomir-124 inhibited Smad2 induction in *in vitro* astrocytes with injury and *in vivo* SCI (Figure S3A−D). As shown in the analysis of the ENCORI database, the binding site between miR-124-3p and the 3′-UTR of Smad2 has been predicted (Figure 4B). Furthermore, the detection of dual-luciferase activity revealed significantly downregulated miR-124-3p expression in miR-124-3p mimic-transfected A172 cells with Smad2-WT but not with Smad2-MUT, confirming the targeting relationship between miR-124-3p and Smad2 (Figure 4B). The miR-124-3p mimic and the miR-124-3p inhibitor successfully overexpressed or interfered with the function of miR-124-3p (Figure 4C). As expected, miR-124-3p overexpression suppressed Smad2, whereas silencing of miR-124-3p activated Smad2 as


https://doi.org/10.1021/acsomega.3c06679
ACS Omega 2024, 9, 781−797

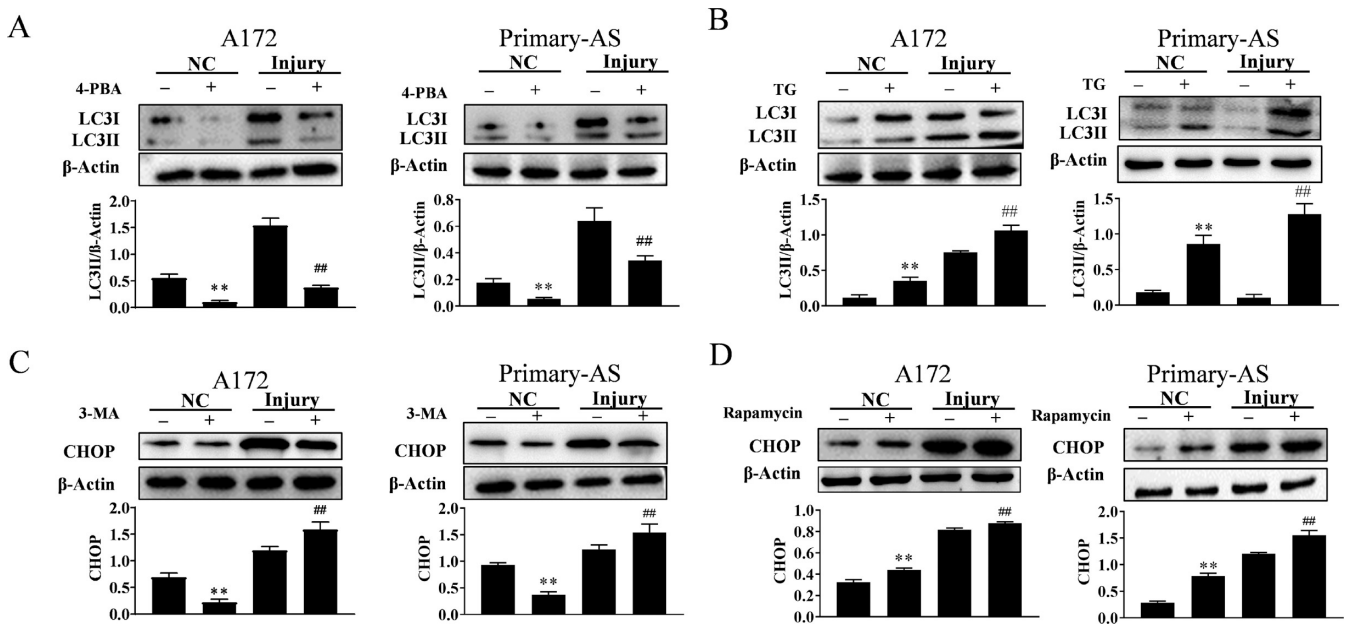


**Figure 7.** Effect of ER stress on autophagy after injury. (A,B) Relative protein levels of LC3II after treatment with an ER stress inhibitor and an ER stress activator in A172 and primary astrocyte cells. (C,D) Relative protein levels of CHOP after treatment with the autophagy inhibitor 3-MA and the autophagy activator rapamycin in A172 and primary astrocyte cells. Mean ± SD, $n = 3$, $^{**}P < 0.01$, $^{\#\#}P < 0.01$. ER, endoplasmic reticulum; SD, standard deviation.

shown in the RT-qPCR and Western blotting results (Figure 4D,E). Injury to A172 cells promoted Smad2 expression, which was blocked by si-circHIPK2 (Figure 4F). circHIPK2 overexpression induced Smad2 expression, but cotransfection of the miR-124-3p mimic significantly decreased Smad2 expression (Figure 4G). The miR-124-3p inhibitor markedly upregulated the Smad2 expression level, which can be significantly downregulated when cotransfected with si-circHIPK2 (Figure 4H). Given that circHIPK2/miR-124-3p might amplify A1 astrocyte expression and directly act on Smad2, we hypothesized that Smad2 plays a critical role in circHIPK2/miR-124-3p-regulated astrocyte function; therefore, we determined the relative expression of C3. In response to injury, C3 was expressed at high levels, but si-Smad2 attenuated the C3 augment (Figure 4I). si-Smad2 treatment also inhibited the high level of C3 induced by the miR-124-3p inhibitor (Figure 4J). C3 expression was reduced by si-circHIPK2 transfection, whereas it was rescued by the miR-124-3p inhibitor and remained at a low level with si-Smad2 cotransfection (Figure 4K).

**circHIPK2/miR-124-3p/Smad2 May Promote the Activation of A1 Astrocytes through Autophagy.** Autophagy was found to be the key mechanism for astrocyte activation. Therefore, after determining that circHIPK2/miR-124-3p/Smad2 induced the activation of the astrocytes, we proceeded to assess the mechanisms of autophagy in astrocytes. Through the analysis of the mRFP−GFP−LC3B fusion series in autophagosome−lysosome fusion in the A172 cell line, we discovered that injury increased autophagy flux but was reversed by Agomir-124 (Figure S4). This indicates that A172 cell injury can induce autophagy. The expression of autophagy-related proteins was examined. LC3II and Beclin-1 levels increased in response to injury in primary astrocytes and the cell line but were downregulated with Agomir-124 treatment (Figure 5A). p62 expression was downregulated in response to injury in primary astrocytes and the cell line but was increased after Agomir-124 treatment. Transfection of cells with si-circHIPK2 (Figure 5B) or si-Smad2 (Figure 5C) profoundly inhibited the injury-mediated LC3II increase in both cell types. The LC3II expression level was downregulated by si-circHIPK2 but reversed by the miR-124-3p inhibitor (Figure 5D). LC3II expression was upregulated in cells cotransfected with the miR-124-3p inhibitor only but downregulated when cells were cotransfected with the miR-124-3p inhibitor and si-Smad2 (Figure 5E). The increases in C3 and LC3II induced by injury were inhibited by the autophagy inhibitor 3-MA (Figure 5F) and further promoted by the autophagy inducer rapamycin (Figure 5G).

**circHIPK2/miR-124-3p/Smad2 May Promote the Activation of A1 Astrocytes through ER Stress.** In addition to autophagy, ER stress is found to be the vital pathway for astrocyte activation. Expression of the ER stress-related proteins GRP78, ATF6$\alpha$, and CHOP and the protein phosphorylation of IRE1$\alpha$ and PERK was upregulated in response to injury in primary astrocytes and the cell line and was downregulated by Agomir-124 treatment (Figure 6A). CHOP expression was blocked by si-circhHIPK2 (Figure 6B) and si-Smad2 (Figure 6C). Transduction of cells with the miR-124-3p inhibitor induced CHOP expression, which might have been attenuated by si-circHIPK2 (Figure 6D) and si-Smad2 (Figure 6E). The ER stress inhibitor 4-PBA limited C3 and CHOP expressions induced by astrocyte injury (Figure 6F). The ER stress agonist thapsigargin (TG, 60 nM) stimulated C3 and CHOP expressions upon induction with cell injury (Figure 6G).

Given that cell injury and astrocyte activation with circHIPK2/miR-124-3p/Smad2 induced both autophagy and ER stress, further research was conducted to ascertain whether ER stress affected autophagy after injury. Pretreatment with 4-PBA caused abrogation of the increase in LC3II induced by injury, and TG evidently upregulated LC3II expression despite the injury (Figure 7A,B). In addition, pretreatment with the


https://doi.org/10.1021/acsomega.3c06679
ACS Omega 2024, 9, 781−797

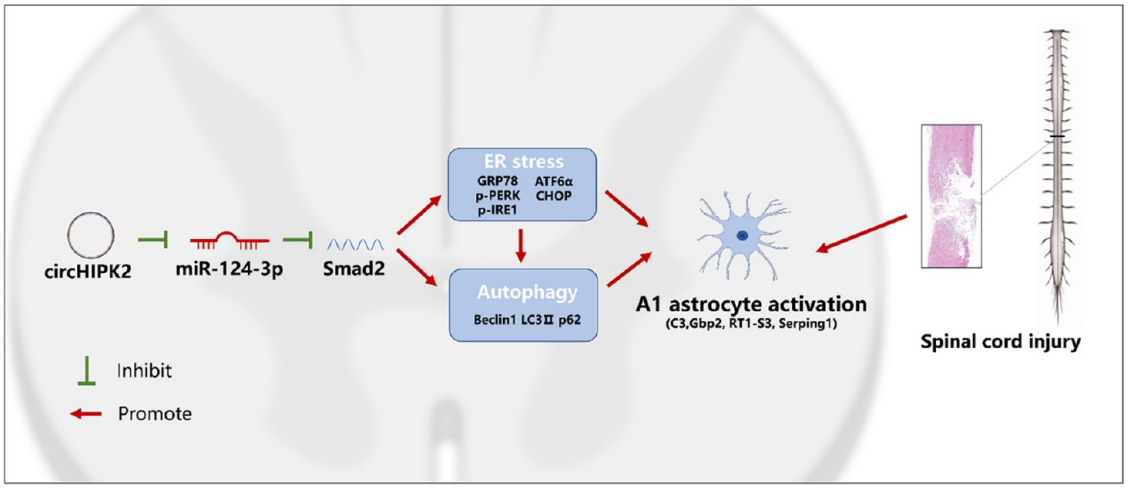


**Figure 8.** Function of miR-124-3p in the activation of A1 astrocytes. miR, micro-RNA.

autophagy inhibitor 3-MA or the autophagy agonist rapamycin led to an increase of CHOP-related expression in injury (Figure 7C,D). This suggests that autophagy may not affect ER stress in injuries. Therefore, ER stress is probably a potent trigger for autophagy in circHIPK2/miR-124-3p/Smad2 that promotes the activation of A1 astrocytes.

## DISCUSSION

There remains a paucity of comprehensive understanding of reactive astrogliosis, even though emerging studies on A1/A2 astrocyte conversion have applied reactive astrogliosis as a therapeutic strategy for various neurological diseases, including Parkinson's disease,[33] Alzheimer's disease,[34] ischemic stroke,[35] and traumatic brain injury.[36,37] It is an imperative pathological process during SCI, and targeted interventions represent an innovative feasible avenue for SCI. Prevention of A1 astrocyte formation or enhancement of A1/A2 astrocyte shift efficiently promotes axonal regeneration and spinal neuronal plasticity after SCI.[4,14,38−40] Thus, it is imperative to uncover the associated mechanisms. In this study, we demonstrated that circRNA HIPK2 enhances A1 astrocyte activation after SCI through autophagy and ER stress by modulating miR-124-3p-dependent Smad2 expression (Figure 8), providing an alternative explanation about the potential mechanism of miR-124-3p's function in astrocyte activation and SCI.

miR-124-3p has emerged as a promising therapeutic target for SCI as it plays a role in modulating neural plasticity and repair. It not only promotes the re-emergence in surviving neurons of a preneuronal phenotype, wherein it promotes neuronal differentiation and migration of spinal cord neural progenitor cells[41] and suppresses neuronal cell apoptosis.[42,43] Microglial exosomes carrying miR-124-3P have neuroprotective effects, reduce neuroinflammation, and promote the repair and plasticity of neurons.[44] According to our unpublished data, miR-124-3p promotes neurite extension, which is consistent with its reported protective effect on SCI by neuronal inflammation inhibition and neurite outgrowth.[45] miR-124-3p inhibits neurite outgrowth in an inflammatory environment.[46] miR-124-3p regulates rat cortical reactive astrocytes into neuron reprogramming[47] and promotes integration between Schwann cells and astrocytes.[48] Currently, there has been a growing body of research implicating the role of miR-124-3p in microglia and astrocyte activation, triggering neuroinflammation response through its targets and associated pathways following SCI.[49] miR-124-3p promotes astrocyte activation in neuroinflammatory diseases[22] and ischemic stroke,[50] and data from our previous study reveal that miR-124-3p inhibits neuronal death and exerts potential therapeutic effects attributable to astrocyte activation.[18] All of these studies measured only the level of pan-reactive transcripts of GFAP, but activated astrocytes are complex with diverse functions and can be differentiated into the A1 and A2 phenotypes.[11] In addition to the increase in pan-reactive transcripts at 14 dpi, A1-specific transcripts start increasing from 3 dpi and continue in the subsequent several weeks, whereas A2-specific transcripts have shown only a slight increase, followed by a reduction at 7 dpi, although controversy is inevitable owing to the unclear definitive markers for A1 or A2 astrocyte activation.[39] Exosome-derived miR-124-3p originating from neurons attenuates M1 microglia and A1 astrocyte activation, thus alleviating inhibitory effects both *in vitro* and *in vivo* to enhance functional recovery.[24] Coincidently, well-studied targets of miR-124, including Notch and NF-κB, participate in A1 astrocyte activation through the Notch-STAT3 and NF-κB/C3/C3aR pathways.[51,52] Therefore, we assumed that miR-124-3p-regulated astrocyte activation mainly refers to the activation of A1 astrocytes, potentially serving as a promising strategy for SCI treatment, as previously demonstrated.

To confirm our prediction on the role of miR-124-3p in A1 astrocyte activation, RNA-Seq was performed on rats of the sham group, SCI group, or Agomir-124 treatment group at 7 dpi, and RT-qPCR and Western blot assays were carried out to ascertain the changes in representative genes under *in vivo* and *in vitro* conditions. The results revealed the upregulated expression of A1 astrocyte-associated markers including C3, Gbp2, RT1-S3, and SerpinG1, with no significant difference in A2 astrocyte-related markers between the SCI and sham groups and downregulation of RT1-S3 with Agomir-124 treatment. The results of RT-qPCR and Western blotting showed a converse expression pattern between A1-specific transcripts and miR-124-3p during injury, and Agomir-124 treatment inhibits A1 astrocyte activation. A1-specific genes were characterized as factors induced by neuroinflammation, while A2-specific genes were characterized as factors that increased in the astrocytes of the ischemia model.[11,53] The inconsistency in the results may have occurred because single


https://doi.org/10.1021/acsomega.3c06679
ACS Omega 2024, 9, 781−797

cells *in vitro* are unable to accurately simulate the intricate physiological processes that occur *in vivo*.

The present study also explored the underlying regulatory mechanisms. circHIPK2 was characterized as being located upstream of miR-124-3p. circRNA selection was based on our sequencing data and public circRNA microarray data (GSE114426) and based on its reported efficacy in the CNS and the confirmed interaction between circHIPK2 and miR-124-3p in some related studies.[22,54−56] Analyzing other potential circular RNAs is beyond the current scope of research. Therefore, we did not pay much attention to the other circRNAs. However, given that circRNA formation competes with the formation of linear cognates, it is speculated that circROCK1 decreases after SCI because linear ROCK1 increases in SCI.[57] Moreover, given that circHIPK2/miR-124-3p/SIGMAR1 plays a role in astrocyte activation in the hippocampus and inflammation of astrocytes induced by methamphetamine,[22] the gut microbiota−circHIPK2 axis regulates astrocyte activity,[58] autophagy-mediated circHIPK2 promotes lipopolysaccharide-induced astrocytic inflammation via SIGMAR1,[59] and we put forward whether circHIPK2/miR-124-3p was involved in the activation of A1 astrocytes in SCI and *in vitro* injury. Our results from two cell types and an *in vivo* SCI model verified the correlation between circHIPK2 and the pathogenesis of SCI, demonstrating that circHIPK2 is an endogenous sponge targeting miR-124-3p, which in turn promotes the activation of A1 astrocytes after SCI.

Since miR-124-3p targets a wide range of molecules, the search was conducted for downstream targets of circHIPK2/miR-124-3p that are involved in the activation of A1 astrocytes. First, by searching the literature, we identified two genes, Elovl and Smad2, that were associated with astrocytes.[60,61] Second, studies have shown one mechanism that miR-124-3p inhibits astrocyte activation or switches the astrocytes into induced neurons, wherein autophagy, ER stress, PI3K/AKT/NF-$\kappa$B, and ARE-mediated mRNA decay signals are considered to be involved.[22,24,62] To establish associations among miR-124-3p, astrocyte activation, and potential target genes, we performed a literature review of the study topic. In astrocytes, Elovl mediates the production of long-chain saturated fatty acids, and Smad2 is associated with autophagy.[60] Therefore, only the following hypothesis is plausible: miR-124-3p/Smad2 axis-mediated autophagy and/or ER stress play roles in astrocyte activation. We also anticipated validating a hypothesis based on as much literature as possible. Therefore, we chose Smad2 for subsequent experiments. We documented that HIPK2/miR-124-3p-mediated A1 astrocytes after SCI were at least partially dependent on promoting Smad2 expression. Smad2 is a signal transducer participating in the TGF-$\beta$ signaling cascade. TGF-$\beta$ increases after SCI onset,[63] and it exacerbates excitotoxicity,[64] inhibits the formation of glial scars, and increases the activation of microglia/macrophages;[65] inhibition of the TGF-$\beta$/Smads facilitates the spinal function of SCI.[66] TGF-$\beta$1 promotes astrocyte secretion and astrogliosis after SCI by upregulating miR-21 expression,[67] which is proven to promote A1 astrocyte polarization through the CNTF/STAT3/Nkrf pathway.[38] TGF-$\beta$3 exerts a neuroprotective effect and alleviates A1-specific marker expression and neurotoxic responses in naive or activated astrocytes to improve neuronal survival.[68] These contradictory results can explain the distinct actions of different types of TGF-$\beta$ depending on the cell type and condition; however, the detailed mechanisms and cellular pathways bridging circHIPK2/miR-124-3p-regulated TGF-$\beta$/Smad signaling to astrocytic reaction/A1-specific markers after SCI require further investigation.

Regulation of astrocyte activation highlights the importance of cooperation between the mechanisms of autophagy and ER stress,[22,69−72] yet it remains unclear whether these coordinated mechanisms orchestrate the expression of A1-type transcripts in response to circHIPK2/miR-124-3p/Smad2 during SCI. There is no dispute that hyperactivation of autophagy,[73] ER stress,[74,75] or ER stress−autophagy axis[71,72] triggers the production of a plethora of proinflammatory molecules closely associated with A1 astrocytes. SCI induces the highest level of ER stress in astrocytes.[76] Our findings demonstrated that si-circHIPK2 inhibited injury-induced ER stress through miR-124-3p/Smad2 to regulate A1 astrocytes, consistent with the findings of previous studies of circHIPK2/miR-124-3p/SIGMAR1 in terms of astrocyte activation.[22] Although studies on astrocytes uncover the enhancement of autophagy by ER stress, autophagy may lead to contrasting outcomes by either inducing[69] or inhibiting[22,71,72] the activation of astrocytes. circHIPK2/miR-124-3p-modulated autophagy also inhibits ER stress in return through SIGMAR1.[22] Because of the inconsistent targets and distinct models of cells or animals, the current study showed that circHIPK2/miR-124-3p triggers autophagy through the Smad2-induced ER stress pathway, finally promoting A1 astrocyte activation during injury. This can be explained by completely different mechanisms of autophagy regulation. An increase in the autophagy initiator Beclin-1 or a decrease in the adapter protein p62 (SQSTM1) would elevate the formation or decrease the degradation of autophagosomes, respectively, causing increased accumulation of LC3II. Modulation of LC3II/LC3I and the p62 protein, which are regulated by LPS or methamphetamine treatment in those investigations as well as in our study, seemed that Beclin-1-dependent autophagy induced the activation of A1 astrocytes. There are heterogeneous autophagic responses caused by SCI in different cell types.[77] The autophagic flux of astrocytes in the spinal cord is extremely low under physiological conditions, which then becomes overactivated at the peripheral injury site at 7 dpi with the accumulation of LC3II and the key protein involved in autophagy initiation (Beclin-1). Increased colocalized staining of GFAP and autophagic markers at the damage border suggests that reactive astrocytes induce a high degree of autophagy activation.[77] We speculated that miR-124-3p induces changes in Beclin-1 and LC3II through different targets, resulting in the inhibition and promotion of autophagic flux;[78,79] finally, the coordinated effects maintain the balance between cell death and astrocyte activation. These findings reveal the detailed molecular mechanism of action of miR-124-3p, which can help to improve subtype-selective therapeutic strategies for SCI.

## CONCLUSIONS

In summary, our research showed that the expression of A1 astrocyte-related markers increased after SCI but reversed after Agomir-124 treatment. circHIPK2 plays a functional role in sequestering miR-124-3p, consequently enabling the facilitation of A1 astrocyte activation through regulating Smad2 and the downstream autophagy and ER stress pathways. The results obtained from this study could offer new perspectives on regulatory mechanisms and potentially assist in the formulation of therapeutic strategies for SCI. The functional significance of circHIPK2/miR-124-3p/Smad2 in mechanisms


https://doi.org/10.1021/acsomega.3c06679
ACS Omega 2024, 9, 781−797

regulating astrocyte activation offers new perspectives for identifying potential targets for functional recovery after SCI.

## ■ ASSOCIATED CONTENT

### Data Availability Statement

The data that support the findings of this study are included in the manuscript and the Supporting Information.

### Supporting Information

The Supporting Information is available free of charge at https://pubs.acs.org/doi/10.1021/acsomega.3c06679.

> Knockdown of circHIPK2 inhibits the related expression of circHIPK2 (Figure S1); knockdown of circHIPK2 inhibits the activation of A1 astrocytes both *in vitro* and *in vivo* (Figure S2); Smad2 expression level with or without Agomir-124 treatment after SCI (Figure S3); the autophagy in the mRFP−GFP−LC3B-transfected A172 cells (Figure S4); the expression of all circRNAs and mRNAs in the rats from Sham and SCI groups (Table S1); circRNA selection based on predicted target circRNAs of miR-124-3p and upregulated circRNAs in spinal cord tissue after injury (Table S2); target genes of miR-124-3p based on target prediction and down-regulated genes after Agomir-124 treatment, and targets in mice and human (Table S3) (PDF)

## ■ AUTHOR INFORMATION


### Corresponding Author

**Lingqiang Chen** − *Department of Orthopedics, The First Affiliated Hospital of Kunming Medical University, Kunming 650032 Yunnan, China*; orcid.org/0000-0002-7194-2009; Phone: +86-13888589986; Email: chenlqkm@sina.com

### Authors

**Jin Yang** − *Department of Orthopedics, The First Affiliated Hospital of Kunming Medical University, Kunming 650032 Yunnan, China*

**Junjie Dong** − *Department of Orthopedics, The First Affiliated Hospital of Kunming Medical University, Kunming 650032 Yunnan, China*

**Haotian Li** − *Department of Orthopedics, The First Affiliated Hospital of Kunming Medical University, Kunming 650032 Yunnan, China*

**Zhiqiang Gong** − *Department of Orthopedics, The First Affiliated Hospital of Kunming Medical University, Kunming 650032 Yunnan, China*

**Bing Wang** − *Department of Orthopedics, The First Affiliated Hospital of Kunming Medical University, Kunming 650032 Yunnan, China*

**Kaili Du** − *Department of Orthopedics, The First Affiliated Hospital of Kunming Medical University, Kunming 650032 Yunnan, China*

**Chunqiang Zhang** − *Department of Orthopedics, The First Affiliated Hospital of Kunming Medical University, Kunming 650032 Yunnan, China*

**Hangchuan Bi** − *Department of Orthopedics, The First Affiliated Hospital of Kunming Medical University, Kunming 650032 Yunnan, China*

**Junfei Wang** − *Department of Orthopedics, The First Affiliated Hospital of Kunming Medical University, Kunming 650032 Yunnan, China*

**Xinpeng Tian** − *Department of Orthopedics, The First Affiliated Hospital of Kunming Medical University, Kunming 650032 Yunnan, China*

Complete contact information is available at: https://pubs.acs.org/10.1021/acsomega.3c06679


### Author Contributions

†J.Y. and J.D. contributed equally to this work, and they were cofirst authors. J.Y. and J.D. performed the experiments and collected the data; they were the major contributors in writing the manuscript and were listed as cofirst authors. H.L., Z.G., B.W., K.D., C.Z., H.B., J.W., and X.T. were responsible for data analysis, data interpretation, visualization, and literature search. L.C. conceived and designed the study, and he was a major contributor in critically revising the manuscript. All authors read and approved the final manuscript.

### Notes

The authors declare no competing financial interest.

## ■ ACKNOWLEDGMENTS

The language of this study was professionally edited by ExEditing.com. This study was supported by the Distinguished Youth Cultivation Program of Associated Project of Yunnan Province Science & Technology Department and Kunming Medical University Basic Research for Application (Grant No.: 202101AY070001-031), the Associated Project of Yunnan Province Science & Technology Department and Kunming Medical University Basic Research for Application [Grant Nos.: 2019FE001(-207) and 2019FE001(-141)], the Project of Yunnan Province Science & Technology Department Basic Research for Application (Grant No.: 202101AT070226), the National Natural Science Foundation of China (NSFC) (Grant Nos.: 81860093 and 81660215), and the Major Science and Technology Project of Yunnan Provincial Department of Science and Technology, Yunnan Provincial Orthopedic and Sports Rehabilitation Clinical Medicine Research Center (Grant No.: 202102AA310068).

## ■ ABBREVIATIONS

SCI:spinal cord injury; miR-124-3p:micro-RNA 124-3p; circRNA:circular ribonucleic acid; CNS:central nervous system; TNF:tumor necrosis factor; IL:interleukin; ER:endoplasmic reticulum; NC:negative control; FBS:fetal bovine serum; DMEM:Dulbecco's modified Eagle's medium; TG:thapsigargin; WT:wild type; MUT:mutant; 4-PBA:4-phenyl butyric acid; UTR:3′-untranslated region; ELISA:enzyme-linked immunosorbent assay

## ■ REFERENCES


(1) Karsy, M.; Hawryluk, G. Modern Medical Management of Spinal Cord Injury. *Curr. Neurol. Neurosci. Rep.* **2019**, *19* (9), No. 65.

(2) Chen, X.; Li, H. Neuronal reprogramming in treating spinal cord injury. *Neural Regen Res.* **2022**, *17* (7), 1440−1445.

(3) Gengatharan, A.; Bammann, R. R.; Saghatelyan, A. The Role of Astrocytes in the Generation, Migration, and Integration of New Neurons in the Adult Olfactory Bulb. *Front. Neurosci.* **2016**, *10*, 149.

(4) Li, X.; Li, M.; Tian, L.; Chen, J.; Liu, R.; Ning, B. Reactive Astrogliosis: Implications in Spinal Cord Injury Progression and Therapy. *Oxid. Med. Cell. Longevity* **2020**, *2020*, No. 9494352.

(5) Okada, S.; Hara, M.; Kobayakawa, K.; Matsumoto, Y.; Nakashima, Y. Astrocyte reactivity and astrogliosis after spinal cord injury. *Neurosci. Res.* **2018**, *126*, 39−43.

(6) Escartin, C.; Galea, E.; Lakatos, A.; O'Callaghan, J. P.; Petzold, G. C.; Serrano-Pozo, A.; Steinhäuser, C.; Volterra, A.; Carmignoto, G.; Agarwal, A.; Allen, N. J.; Araque, A.; Barbeito, L.; Barzilai, A.; Bergles, D. E.; Bonvento, G.; Butt, A. M.; Chen, W. T.; Cohen-Salmon, M.; Cunningham, C.; Deneen, B.; De Strooper, B.; Díaz-Castro, B.; Farina, C.; Freeman, M.; Gallo, V.; Goldman, J. E.; Goldman, S. A.; Götz, M.; Gutiérrez, A.; Haydon, P. G.; Heiland, D. H.; Hol, E. M.; Holt, M. G.; Iino, M.; Kastanenka, K. V.; Kettenmann, H.; Khakh, B. S.; Koizumi, S.; Lee, C. J.; Liddelow, S. A.; MacVicar, B. A.; Magistretti, P.; Messing, A.; Mishra, A.; Molofsky, A. V.; Murai, K. K.; Norris, C. M.; Okada, S.; Oliet, S. H. R.; Oliveira, J. F.; Panatier, A.; Parpura, V.; Pekna, M.; Pekny, M.; Pellerin, L.; Perea, G.; Pérez-Nievas, B. G.; Pfrieger, F. W.; Poskanzer, K. E.; Quintana, F. J.; Ransohoff, R. M.; Riquelme-Perez, M.; Robel, S.; Rose, C. R.; Rothstein, J. D.; Rouach, N.; Rowitch, D. H.; Semyanov, A.; Sirko, S.; Sontheimer, H.; Swanson, R. A.; Vitorica, J.; Wanner, I. B.; Wood, L. B.; Wu, J.; Zheng, B.; Zimmer, E. R.; Zorec, R.; Sofroniew, M. V.; Verkhratsky, A. Reactive astrocyte nomenclature, definitions, and future directions. *Nat. Neurosci.* **2021**, *24* (3), 312−325.

(7) Cregg, J. M.; DePaul, M. A.; Filous, A. R.; Lang, B. T.; Tran, A.; Silver, J. Functional regeneration beyond the glial scar. *Exp. Neurol.* **2014**, *253*, 197−207.

(8) Fan, H.; Zhang, K.; Shan, L.; Kuang, F.; Chen, K.; Zhu, K.; Ma, H.; Ju, G.; Wang, Y. Z. Reactive astrocytes undergo M1 microglia/macrohpages-induced necroptosis in spinal cord injury. *Mol. Neurodegener.* **2016**, *11*, No. 14.

(9) Bradbury, E. J.; Burnside, E. R. Moving beyond the glial scar for spinal cord repair. *Nat. Commun.* **2019**, *10* (1), No. 3879.

(10) Liddelow, S. A.; Barres, B. A. Reactive Astrocytes: Production, Function, and Therapeutic Potential. *Immunity* **2017**, *46* (6), 957−967.

(11) Liddelow, S. A.; Guttenplan, K. A.; Clarke, L. E.; Bennett, F. C.; Bohlen, C. J.; Schirmer, L.; Bennett, M. L.; Münch, A. E.; Chung, W. S.; Peterson, T. C.; Wilton, D. K.; Frouin, A.; Napier, B. A.; Panicker, N.; Kumar, M.; Buckwalter, M. S.; Rowitch, D. H.; Dawson, V. L.; Dawson, T. M.; Stevens, B.; Barres, B. A. Neurotoxic reactive astrocytes are induced by activated microglia. *Nature* **2017**, *541* (7638), 481−487.

(12) Guttenplan, K. A.; Weigel, M. K.; Prakash, P.; Wijewardhane, P. R.; Hasel, P.; Rufen-Blanchette, U.; Münch, A. E.; Blum, J. A.; Fine, J.; Neal, M. C.; Bruce, K. D.; Gitler, A. D.; Chopra, G.; Liddelow, S. A.; Barres, B. A. Neurotoxic reactive astrocytes induce cell death via saturated lipids. *Nature* **2021**, *599* (7883), 102−107.

(13) Kwon, H. S.; Koh, S. H. Neuroinflammation in neurodegenerative disorders: the roles of microglia and astrocytes. *Transl. Neurodegener.* **2020**, *9* (1), No. 42.

(14) Vismara, I.; Papa, S.; Veneruso, V.; Mauri, E.; Mariani, A.; De Paola, M.; Affatato, R.; Rossetti, A.; Sponchioni, M.; Moscatelli, D.; Sacchetti, A.; Rossi, F.; Forloni, G.; Veglianese, P. Selective Modulation of A1 Astrocytes by Drug-Loaded Nano-Structured Gel in Spinal Cord Injury. *ACS Nano* **2020**, *14* (1), 360−371.

(15) Liu, W.; Wang, Y.; Gong, F.; Rong, Y.; Luo, Y.; Tang, P.; Zhou, Z.; Zhou, Z.; Xu, T.; Jiang, T.; Yang, S.; Yin, G.; Chen, J.; Fan, J.; Cai, W. Exosomes Derived from Bone Mesenchymal Stem Cells Repair Traumatic Spinal Cord Injury by Suppressing the Activation of A1 Neurotoxic Reactive Astrocytes. *J. Neurotrauma* **2019**, *36* (3), 469−484.

(16) Zhang, Q.; Liu, C.; Shi, R.; Zhou, S.; Shan, H.; Deng, L.; Chen, T.; Guo, Y.; Zhang, Z.; Yang, G. Y.; Wang, Y.; Tang, Y. Blocking C3d(+)/GFAP(+) A1 Astrocyte Conversion with Semaglutide Attenuates Blood-Brain Barrier Disruption in Mice after Ischemic Stroke. *Aging Dis.* **2022**, *13* (3), 943−959.

(17) Han, D.; Dong, X.; Zheng, D.; Nao, J. MiR-124 and the Underlying Therapeutic Promise of Neurodegenerative Disorders. *Front. Pharmacol.* **2020**, *10*, 1555.

(18) Wang, J.; Li, H.; Chen, L.; Dong, J.; Yang, J.; Gong, Z.; Wang, B.; Zhao, X. mRNA Profiling for miR-124-mediated Repair in Spinal Cord Injury. *Neuroscience* **2020**, *438*, 158−168.

(19) Zhao, Y.; Zhang, H.; Zhang, D.; Yu, C. Y.; Zhao, X. H.; Liu, F. F.; Bian, G. L.; Ju, G.; Wang, J. Loss of microRNA-124 expression in neurons in the peri-lesion area in mice with spinal cord injury. *Neural Regen Res.* **2015**, *10* (7), 1147−1152.

(20) Guo, Y.; Hong, W.; Wang, X.; Zhang, P.; Körner, H.; Tu, J.; Wei, W. MicroRNAs in Microglia: How do MicroRNAs Affect Activation, Inflammation, Polarization of Microglia and Mediate the Interaction Between Microglia and Glioma? *Front. Mol. Neurosci.* **2019**, *12*, 125.

(21) Chen, J.; Fu, B.; Bao, J.; Su, R.; Zhao, H.; Liu, Z. Novel circular RNA 2960 contributes to secondary damage of spinal cord injury by sponging miRNA-124. *J. Comp. Neurol.* **2021**, *529* (7), 1456−1464.

(22) Huang, R.; Zhang, Y.; Han, B.; Bai, Y.; Zhou, R.; Gan, G.; Chao, J.; Hu, G.; Yao, H. Circular RNA HIPK2 regulates astrocyte activation via cooperation of autophagy and ER stress by targeting MIR124−2HG. *Autophagy* **2017**, *13* (10), 1722−1741.

(23) Veremeyko, T.; Kuznetsova, I. S.; Dukhinova, M.; A W, Y. Y.; Kopeikina, E.; Barteneva, N. S.; Ponomarev, E. D. Neuronal extracellular microRNAs miR-124 and miR-9 mediate cell-cell communication between neurons and microglia. *J. Neurosci. Res.* **2019**, *97* (2), 162−184.

(24) Jiang, D.; Gong, F.; Ge, X.; Lv, C.; Huang, C.; Feng, S.; Zhou, Z.; Rong, Y.; Wang, J.; Ji, C.; Chen, J.; Zhao, W.; Fan, J.; Liu, W.; Cai, W. Neuron-derived exosomes-transmitted miR-124-3p protect traumatically injured spinal cord by suppressing the activation of neurotoxic microglia and astrocytes. *J. Nanobiotechnol.* **2020**, *18* (1), No. 105.

(25) Hamzei Taj, S.; Kho, W.; Riou, A.; Wiedermann, D.; Hoehn, M. MiRNA-124 induces neuroprotection and functional improvement after focal cerebral ischemia. *Biomaterials* **2016**, *91*, 151−165.

(26) Jeck, W. R.; Sharpless, N. E. Detecting and characterizing circular RNAs. *Nat. Biotechnol.* **2014**, *32* (5), 453−461.

(27) Ma, X.; Wang, X.; Ma, X.; Zhang, X.; Gong, X.; Sun, R.; Wong, S. H.; Chan, M. T. V.; Wu, W. K. K. An update on the roles of circular RNAs in spinal cord injury. *Mol. Neurobiol.* **2022**, *59* (4), 2620−2628.

(28) Chen, L. L. The biogenesis and emerging roles of circular RNAs. *Nat. Rev. Mol. Cell Biol.* **2016**, *17* (4), 205−211.

(29) Bie, F.; Wang, K.; Xu, T.; Yuan, J.; Ding, H.; Lv, B.; Liu, Y.; Lan, M. The potential roles of circular RNAs as modulators in traumatic spinal cord injury. *Biomed. Pharmacother.* **2021**, *141*, No. 111826.

(30) Liu, J.; Du, L. PERK pathway is involved in oxygen-glucose-serum deprivation-induced NF-kB activation via ROS generation in spinal cord astrocytes. *Biochem. Biophys. Res. Commun.* **2015**, *467* (2), 197−203.

(31) Mandell, J. W.; Gocan, N. C.; Vandenberg, S. R. Mechanical trauma induces rapid astroglial activation of ERK/MAP kinase: Evidence for a paracrine signal. *Glia* **2001**, *34* (4), 283−295.

(32) Yi, M.; Dou, F.; Lu, Q.; Yu, Z.; Chen, H. Activation of the KCa3.1 channel contributes to traumatic scratch injury-induced reactive astrogliosis through the JNK/c-Jun signaling pathway. *Neurosci. Lett.* **2016**, *624*, 62−71.

(33) Yun, S. P.; Kam, T. I.; Panicker, N.; Kim, S.; Oh, Y.; Park, J. S.; Kwon, S. H.; Park, Y. J.; Karuppagounder, S. S.; Park, H.; Kim, S.; Oh, N.; Kim, N. A.; Lee, S.; Brahmachari, S.; Mao, X.; Lee, J. H.; Kumar, M.; An, D.; Kang, S. U.; Lee, Y.; Lee, K. C.; Na, D. H.; Kim, D.; Lee, S. H.; Roschke, V. V.; Liddelow, S. A.; Mari, Z.; Barres, B. A.; Dawson, V. L.; Lee, S.; Dawson, T. M.; Ko, H. S. Block of A1 astrocyte conversion by microglia is neuroprotective in models of Parkinson's disease. *Nat. Med.* **2018**, *24* (7), 931−938.

(34) King, A.; Szekely, B.; Calapkulu, E.; Ali, H.; Rios, F.; Jones, S.; Troakes, C. The Increased Densities, But Different Distributions, of Both C3 and S100A10 Immunopositive Astrocyte-Like Cells in Alzheimer's Disease Brains Suggest Possible Roles for Both A1 and A2 Astrocytes in the Disease Pathogenesis. *Brain Sci.* **2020**, *10* (8), 503.

(35) Guo, H.; Fan, Z.; Wang, S.; Ma, L.; Wang, J.; Yu, D.; Zhang, Z.; Wu, L.; Peng, Z.; Liu, W.; Hou, W.; Cai, Y. Astrocytic A1/A2 paradigm participates in glycogen mobilization mediated neuro-



https://doi.org/10.1021/acsomega.3c06679
*ACS Omega* 2024, 9, 781−797

protection on reperfusion injury after ischemic stroke. *J. Neuroinflammation* **2021**, *18* (1), No. 230.
(36) Clark, D. P. Q.; Perreau, V. M.; Shultz, S. R.; Brady, R. D.; Lei, E.; Dixit, S.; Taylor, J. M.; Beart, P. M.; Boon, W. C. Inflammation in Traumatic Brain Injury: Roles for Toxic A1 Astrocytes and Microglial-Astrocytic Crosstalk. *Neurochem. Res.* **2019**, *44* (6), 1410−1424.
(37) Zou, H. J.; Guo, S. W.; Zhu, L.; Xu, X.; Liu, J. B. Methylprednisolone Induces Neuro-Protective Effects via the Inhibition of A1 Astrocyte Activation in Traumatic Spinal Cord Injury Mouse Models. *Front. Neurosci.* **2021**, *15*, No. 628917.
(38) Zhang, Y.; Meng, T.; Chen, J.; Zhang, Y.; Kang, J.; Li, X.; Yu, G.; Tian, L.; Jin, Z.; Dong, H.; Zhang, X.; Ning, B. miR-21a-5p Promotes Inflammation following Traumatic Spinal Cord Injury through Upregulation of Neurotoxic Reactive Astrocyte (A1) Polarization by Inhibiting the CNTF/STAT3/Nkrf Pathway. *Int. J. Biol. Sci.* **2021**, *17* (11), 2795−2810.
(39) Wang, X.; Zhang, Z.; Zhu, Z.; Liang, Z.; Zuo, X.; Ju, C.; Song, Z.; Li, X.; Hu, X.; Wang, Z. Photobiomodulation Promotes Repair Following Spinal Cord Injury by Regulating the Transformation of A1/A2 Reactive Astrocytes. *Front. Neurosci.* **2021**, *15*, No. 768262.
(40) Li, L.; Li, Y.; He, B.; Li, H.; Ji, H.; Wang, Y.; Zhu, Z.; Hu, Y.; Zhou, Y.; Yang, T.; Sun, C.; Yuan, Y.; Wang, Y. HSF1 is involved in suppressing A1 phenotype conversion of astrocytes following spinal cord injury in rats. *J. Neuroinflammation* **2021**, *18* (1), No. 205.
(41) Cui, Y.; Yin, Y.; Xiao, Z.; Zhao, Y.; Chen, B.; Yang, B.; Xu, B.; Song, H.; Zou, Y.; Ma, X.; Dai, J. LncRNA Neat1 mediates miR-124-induced activation of Wnt/$\beta$-catenin signaling in spinal cord neural progenitor cells. *Stem Cell Res. Ther.* **2019**, *10* (1), No. 400.
(42) Xu, Z.; Zhang, K.; Wang, Q.; Zheng, Y. MicroRNA-124 improves functional recovery and suppresses Bax-dependent apoptosis in rats following spinal cord injury. *Mol. Med. Rep.* **2019**, *19* (4), 2551−2560.
(43) Yuan, S.; Wang, Y. X.; Gong, P. H.; Meng, C. Y. MiR-124 inhibits spinal neuronal apoptosis through binding to GCH1. *Eur. Rev. Med. Pharmacol. Sci.* **2019**, *23* (11), 4564−4574.
(44) Mavroudis, I.; Balmus, I. M.; Ciobica, A.; Nicoara, M. N.; Luca, A. C.; Palade, D. O. The Role of Microglial Exosomes and miR-124-3p in Neuroinflammation and Neuronal Repair after Traumatic Brain Injury. *Life* **2023**, *13* (9). 1924.
(45) Huang, S.; Ge, X.; Yu, J.; Han, Z.; Yin, Z.; Li, Y.; Chen, F.; Wang, H.; Zhang, J.; Lei, P. Increased miR-124-3p in microglial exosomes following traumatic brain injury inhibits neuronal inflammation and contributes to neurite outgrowth via their transfer into neurons. *FASEB J.* **2018**, *32* (1), 512−528.
(46) Hartmann, H.; Hoehne, K.; Rist, E.; Louw, A. M.; Schlosshauer, B. miR-124 disinhibits neurite outgrowth in an inflammatory environment. *Cell Tissue Res.* **2015**, *362* (1), 9−20.
(47) Zheng, Y.; Huang, Z.; Xu, J.; Hou, K.; Yu, Y.; Lv, S.; Chen, L.; Li, Y.; Quan, C.; Chi, G. MiR-124 and Small Molecules Synergistically Regulate the Generation of Neuronal Cells from Rat Cortical Reactive Astrocytes. *Mol. Neurobiol.* **2021**, *58* (5), 2447−2464.
(48) Li, Z.; Yu, Y.; Kang, J.; Zheng, Y.; Xu, J.; Xu, K.; Hou, K.; Hou, Y.; Chi, G. MicroRNA-124 Overexpression in Schwann Cells Promotes Schwann Cell-Astrocyte Integration and Inhibits Glial Scar Formation Ability. *Front. Cell Neurosci.* **2020**, *14*, 144.
(49) Xu, J.; Zheng, Y.; Wang, L.; Liu, Y.; Wang, X.; Li, Y.; Chi, G. miR-124: A Promising Therapeutic Target for Central Nervous System Injuries and Diseases. *Cell Mol. Neurobiol.* **2022**, *42*, 2031.
(50) Li, Z.; Song, Y.; He, T.; Wen, R.; Li, Y.; Chen, T.; Huang, S.; Wang, Y.; Tang, Y.; Shen, F.; Tian, H. L.; Yang, G. Y.; Zhang, Z. M2 microglial small extracellular vesicles reduce glial scar formation via the miR-124/STAT3 pathway after ischemic stroke in mice. *Theranostics* **2021**, *11* (3), 1232−1248.
(51) Lian, H.; Yang, L.; Cole, A.; Sun, L.; Chiang, A. C.; Fowler, S. W.; Shim, D. J.; Rodriguez-Rivera, J.; Taglialatela, G.; Jankowsky, J. L.; Lu, H. C.; Zheng, H. NFκB-activated astroglial release of complement C3 compromises neuronal morphology and function associated with Alzheimer's disease. *Neuron* **2015**, *85* (1), 101−115.
(52) Qian, D.; Li, L.; Rong, Y.; Liu, W.; Wang, Q.; Zhou, Z.; Gu, C.; Huang, Y.; Zhao, X.; Chen, J.; Fan, J.; Yin, G. Blocking Notch signal pathway suppresses the activation of neurotoxic A1 astrocytes after spinal cord injury. *Cell Cycle* **2019**, *18* (21), 3010−3029.
(53) Zamanian, J. L.; Xu, L.; Foo, L. C.; Nouri, N.; Zhou, L.; Giffard, R. G.; Barres, B. A. Genomic analysis of reactive astrogliosis. *J. Neurosci.* **2012**, *32* (18), 6391−6410.
(54) Li, S.; Ma, Y.; Tan, Y.; Ma, X.; Zhao, M.; Chen, B.; Zhang, R.; Chen, Z.; Wang, K. Profiling and functional analysis of circular RNAs in acute promyelocytic leukemia and their dynamic regulation during all-trans retinoic acid treatment. *Cell Death Dis.* **2018**, *9* (6), No. 651.
(55) Chen, X.-J.; Zhang, Z.-C.; Wang, X.-Y.; Zhao, H.-Q.; Li, M.-L.; Ma, Y.; Ji, Y.-Y.; Zhang, C.-J.; Wu, K.-C.; Xiang, L.; Sun, L.-F.; Zhou, M.; Jin, Z.-B. The Circular RNome of Developmental Retina in Mice. *Mol. Ther. Nucleic Acids* **2020**, *19*, 339−349.
(56) Wang, G.; Han, B.; Shen, L.; Wu, S.; Yang, L.; Liao, J.; Wu, F.; Li, M.; Leng, S.; Zang, F.; Zhang, Y.; Bai, Y.; Mao, Y.; Chen, B.; Yao, H. Corrigendum to 'Silencing of circular RNA HIPK2 in neural stem cells enhances functional recovery following ischaemic stroke' [EBioMedicine 52 (2020) 102660]. *EBioMedicine* **2020**, *55*, No. 102751.
(57) Li, C.; Sahu, S.; Kou, G.; Jagadeesan, N.; Joseph, T. P.; Li Lin, S.; Schachner, M. Chondroitin 6-sulfate-binding peptides improve recovery in spinal cord-injured mice. *Eur. J. Pharmacol.* **2021**, *910*, No. 174421.
(58) Zhang, Y.; Huang, R.; Cheng, M.; Wang, L.; Chao, J.; Li, J.; Zheng, P.; Xie, P.; Zhang, Z.; Yao, H. Gut microbiota from NLRP3-deficient mice ameliorates depressive-like behaviors by regulating astrocyte dysfunction via circHIPK2. *Microbiome* **2019**, *7* (1), No. 116.
(59) Huang, R.; Cai, L.; Ma, X.; Shen, K. Autophagy-mediated circHIPK2 promotes lipopolysaccharide-induced astrocytic inflammation via SIGMAR1. *Int. Immunopharmacol.* **2023**, *117*, No. 109907.
(60) Siddiqui, A. J.; Jahan, S.; Chaturvedi, S.; Siddiqui, M. A.; Alshahrani, M. M.; Abdelgadir, A.; Hamadou, W. S.; Saxena, J.; Sundararaj, B. K.; Snoussi, M.; et al. Therapeutic Role of ELOVL in Neurological Diseases. *ACS Omega* **2023**, *8* (11), 9764−9774.
(61) Zheng, J. Y.; Sun, J.; Ji, C. M.; Shen, L.; Chen, Z. J.; Xie, P.; Sun, Y. Z.; Yu, R. T. Selective deletion of apolipoprotein E in astrocytes ameliorates the spatial learning and memory deficits in Alzheimer's disease (APP/PS1) mice by inhibiting TGF-$\beta$/Smad2/STAT3 signaling. *Neurobiol. Aging* **2017**, *54*, 112−132.
(62) Papadimitriou, E.; Koutsoudaki, P. N.; Thanou, I.; Karamitros, T.; Karagkouni, D.; Chroni-Tzartou, D.; Gaitanou, M.; Gkemisis, C.; Margariti, M.; Xingi, E.; et al. A miR-124-mediated post-transcriptional mechanism controlling the cell fate switch of astrocytes to induced neurons. *Stem Cell Rep.* **2020**, 915−935, DOI: 10.1016/j.stemcr.2023.02.009.
(63) Ritz, M.-F.; Graumann, U.; Gutierrez, B.; Hausmann, O. Traumatic spinal cord injury alters angiogenic factors and TGF-beta1 that may affect vascular recovery. *Curr. Neurovasc. Res.* **2010**, *7* (4), 301−310.
(64) Mesplès, B.; Fontaine, R. H.; Lelièvre, V.; Launay, J. M.; Gressens, P. Neuronal TGF-beta1 mediates IL-9/mast cell interaction and exacerbates excitotoxicity in newborn mice. *Neurobiol. Dis.* **2005**, *18* (1), 193−205.
(65) Kohta, M.; Kohmura, E.; Yamashita, T. Inhibition of TGF-beta1 promotes functional recovery after spinal cord injury. *Neurosci Res.* **2009**, *65* (4), 393−401.
(66) Lv, C.; Zhang, T.; Li, K.; Gao, K. Bone marrow mesenchymal stem cells improve spinal function of spinal cord injury in rats via TGF-$\beta$/Smads signaling pathway. *Exp. Ther. Med.* **2020**, *19* (6), 3657−3663.
(67) Liu, R.; Wang, W.; Wang, S.; Xie, W.; Li, H.; Ning, B. microRNA-21 regulates astrocytic reaction post-acute phase of spinal cord injury through modulating TGF-$\beta$ signaling. *Aging* **2018**, *10* (6), 1474−1488.
(68) Gottipati, M. K.; D'Amato, A. R.; Ziemba, A. M.; Popovich, P. G.; Gilbert, R. J. TGF$\beta$3 is neuroprotective and alleviates the

neurotoxic response induced by aligned poly-l-lactic acid fibers on naïve and activated primary astrocytes. *Acta Biomater.* **2020**, *117*, 273−282.
(69) Han, B.; Zhang, Y.; Zhang, Y.; Bai, Y.; Chen, X.; Huang, R.; Wu, F.; Leng, S.; Chao, J.; Zhang, J. H.; Hu, G.; Yao, H. Novel insight into circular RNA HECTD1 in astrocyte activation via autophagy by targeting MIR142-TIPARP: implications for cerebral ischemic stroke. *Autophagy* **2018**, *14* (7), 1164−1184.
(70) Thangaraj, A.; Sil, S.; Tripathi, A.; Chivero, E. T.; Periyasamy, P.; Buch, S. Targeting endoplasmic reticulum stress and autophagy as therapeutic approaches for neurological diseases. *Int. Rev. Cell Mol. Biol.* **2020**, *350*, 285−325.
(71) Periyasamy, P.; Guo, M. L.; Buch, S. Cocaine induces astrocytosis through ER stress-mediated activation of autophagy. *Autophagy* **2016**, *12* (8), 1310−1329.
(72) Sil, S.; Periyasamy, P.; Guo, M. L.; Callen, S.; Buch, S. Morphine-Mediated Brain Region-Specific Astrocytosis Involves the ER Stress-Autophagy Axis. *Mol. Neurobiol.* **2018**, *55* (8), 6713−6733.
(73) Sher, A. A.; Gao, A.; Coombs, K. M. Autophagy Modulators Profoundly Alter the Astrocyte Cellular Proteome. *Cells* **2020**, *9* (4). 805.
(74) Reverendo, M.; Mendes, A.; Argüello, R. J.; Gatti, E.; Pierre, P. At the crossway of ER-stress and proinflammatory responses. *FEBS J.* **2019**, *286* (2), 297−310.
(75) Chaumonnot, K.; Masson, S.; Sikner, H.; Bouchard, A.; Baverel, V.; Bellaye, P. S.; Collin, B.; Garrido, C.; Kohli, E. The HSP GRP94 interacts with macrophage intracellular complement C3 and impacts M2 profile during ER stress. *Cell Death Dis.* **2021**, *12* (1), No. 114.
(76) Matsuyama, D.; Watanabe, M.; Suyama, K.; Kuroiwa, M.; Mochida, J. Endoplasmic reticulum stress response in the rat contusive spinal cord injury model-susceptibility in specific cell types. *Spinal Cord* **2014**, *52* (1), 9−16.
(77) Muñoz-Galdeano, T.; Reigada, D.; Del Águila, Á.; Velez, I.; Caballero-López, M. J.; Maza, R. M.; Nieto-Díaz, M. Cell Specific Changes of Autophagy in a Mouse Model of Contusive Spinal Cord Injury. *Front. Cell Neurosci.* **2018**, *12*, 164.
(78) Chen, X.; Mao, R.; Su, W.; Yang, X.; Geng, Q.; Guo, C.; Wang, Z.; Wang, J.; Kresty, L. A.; Beer, D. G.; Chang, A. C.; Chen, G. Circular RNA circHIPK3 modulates autophagy via MIR124-3p-STAT3-PRKAA/AMPK$\alpha$ signaling in STK11 mutant lung cancer. *Autophagy* **2020**, *16* (4), 659−671.
(79) Mehta, A. K.; Hua, K.; Whipple, W.; Nguyen, M. T.; Liu, C. T.; Haybaeck, J.; Weidhaas, J.; Settleman, J.; Singh, A. Regulation of autophagy, NF-$\kappa$B signaling, and cell viability by miR-124 in KRAS mutant mesenchymal-like NSCLC cells. *Sci. Signaling* **2017**, *10* (496), No. eaam6291, DOI: 10.1126/scisignal.aam6291.


https://doi.org/10.1021/acsomega.3c06679
*ACS Omega* 2024, 9, 781−797